Plasma-Material Interactions (PMI) in Magnetic Fusion

G.R. Tynan Guest Lecture
Physics 218C June 2021

Outline:

1. Sketch of the "Problem"
2. PMI: effect of materials on the plasma
   a. Open Field Line Zone - S.O.L.
   b. Plasma Sheaths
   c. Impurities & Neutral Gas
3. PMI: effect of plasma on the material surfaces

(cont'd ↓)

3) PMI: effects of plasma on materials

a) Erosion via Physical, Chemical Sputtering

b) Plasma Ion Implantation & Diffusion, Trapping in Mat'l

c) Evolution / Degradation of Mat'l Properties

d) Heat Flux

4) Frontier Issues

a) Handling Heat Flux @ Divertor Target

- Detached / Radiative Divertor
- Negative Tri-Angularity
- Super-X
- Snowflake Divertor

b) Integrating (a) w/ High Perf. Core Plasma

4b (cont'd)

- adequate β
- low disruption provability
- n/n_G density limit
- No transient First Wall Coating (B, Li, ...)

c) Tritium Retention in Wall & Achieving TBR > 1

[Tritium Breeding Ratio]

d) Adequate First Wall & Diverter Lifetime

- Novel Solid Matl's ⊕ Adequately Small Heat Fluxes
- Liquid Walls ?
  Flowing ?
  Stagnant layer ?
- "Spongy Solid" w/ Liquid Metal Embedded ?

Schematic of the Fusion PMI Problem:

[n.b. discussion focussed on tokamaks, but similar for Stellarators & other magnetic conf. systems]

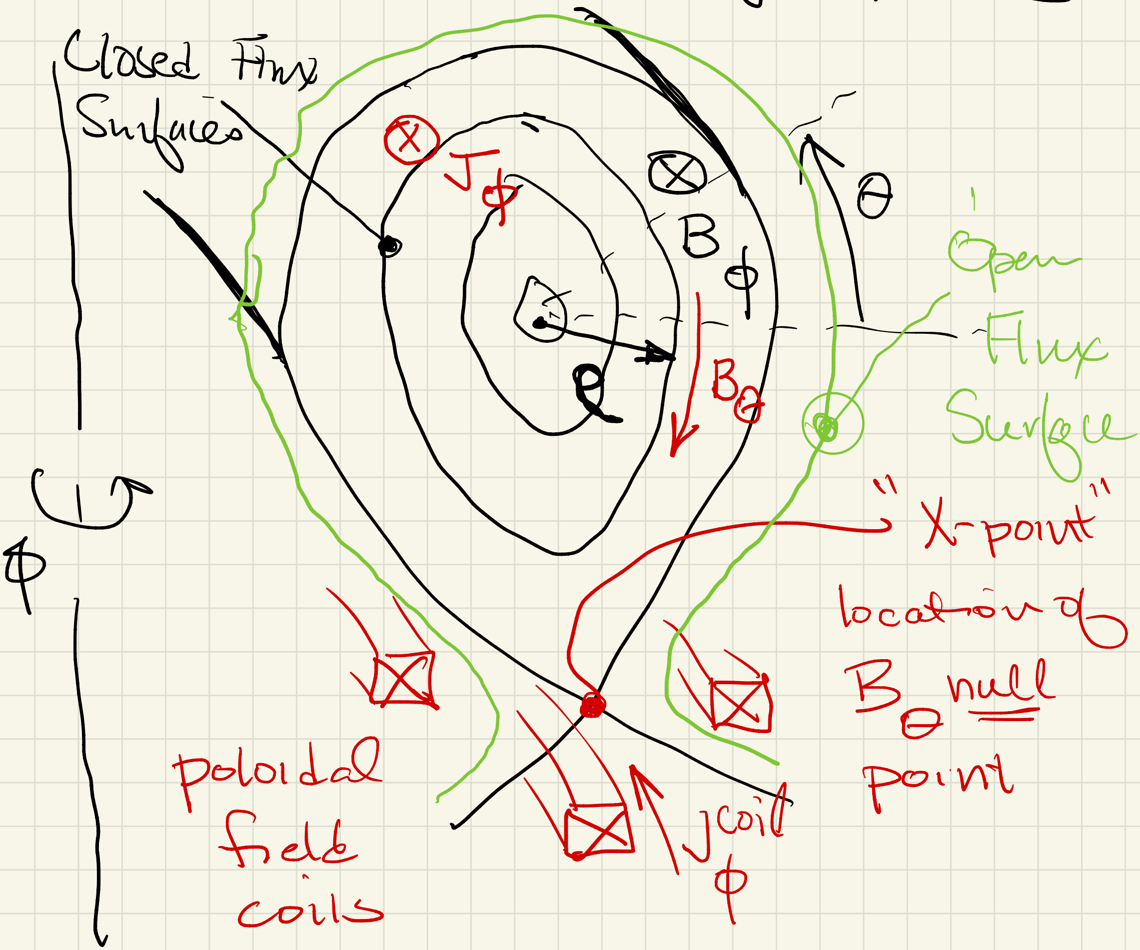

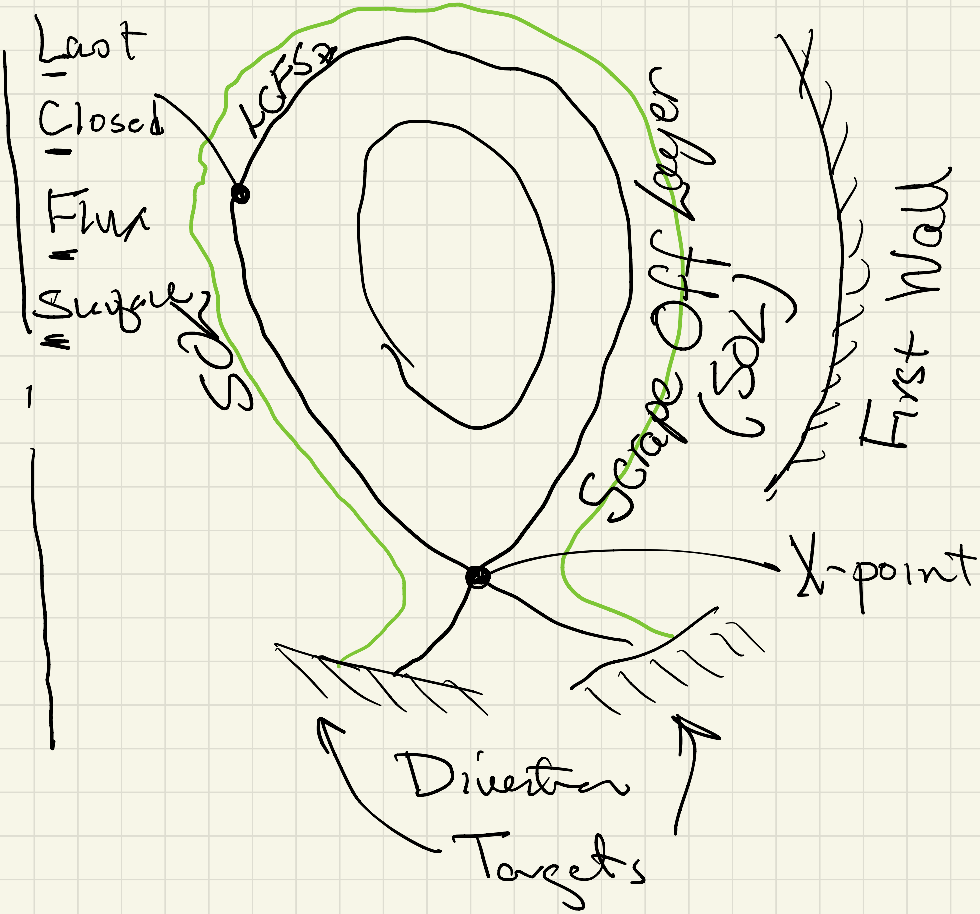

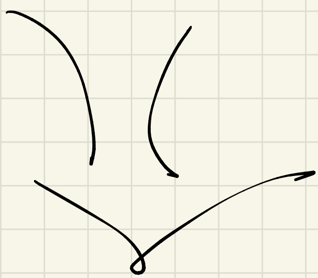

Simplified Representation

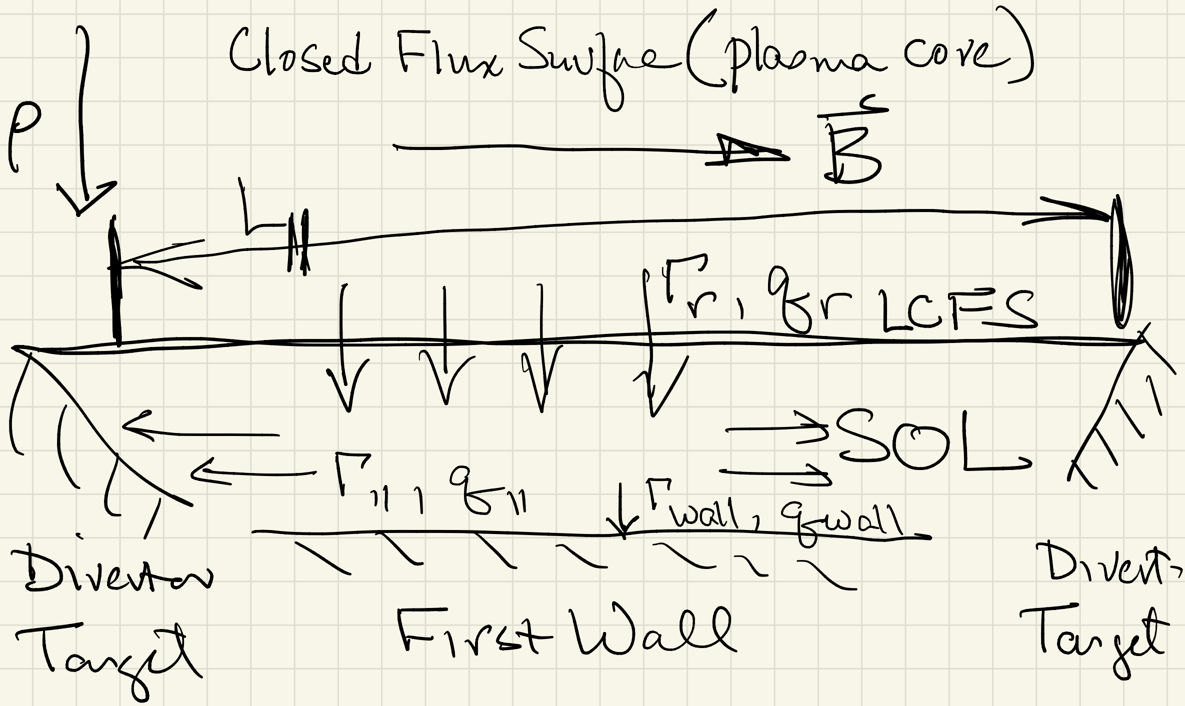

Radial Particle / Heat fluxes $\sim \Gamma_r, q_{e,i\,r}$

$$\Gamma_r \simeq \langle \tilde{n}\, \tilde{v}_r \rangle + \Gamma_r^{neo.}$$

$$q_{e,i\,r} \simeq \frac{3}{2} T_{e,i} \langle \tilde{n}\, \tilde{v}_r \rangle + \frac{3}{2} n_{i,e} \langle \tilde{T}_{e,i}\, \tilde{v}_r \rangle + q^{neo}_{e,i}$$

<u>Question</u>: Once plasma crosses into SOL, what happens to e.g. $n(r)$, $T(r)$, ... ?

lets look at particles: in steady state have

$$\cancel{\frac{\partial n}{\partial t}}^{0} + \bar{\nabla}\cdot\bar{\Gamma} = S_{ion} - R_{recomb} \to$$

Assume Small to make things easy

$$\bar{\nabla}\cdot\bar{\Gamma} = 0$$

or

$$\partial_r \Gamma_r = -\partial_{\parallel}\Gamma_{\parallel}$$

$(n \sim n_0 e^{-r/\lambda_n})$

If $\Gamma_r = -D_{turb}\nabla_r \bar{n} \sim -D_{turb}\dfrac{\bar{n}}{\lambda_n}$

[n.b. SOL transport isn't diffusive!]

// particle transport is convective

$$\Gamma_{//} \simeq \alpha n C_s \qquad 0 < \alpha < 1$$

$C_s \sim$ Ion Acoustic Speed

$$\nabla_{//} \sim \frac{1}{L_{//}} \sim \frac{1}{qR_0}$$

then $\nabla \cdot \vec{\Gamma} = 0 \implies$

$$+ D_{turb} \frac{\cancel{n}}{\lambda_n^2} = + \frac{\alpha \cancel{n} C_s}{qR_0}$$

Solve for λ_n:

$$\lambda_n^2 = \frac{D_{turb} q R_0}{\alpha C_s} \qquad \frac{\frac{m^2}{s} (\cdot)\, m}{(\cdot)\, m/s} \sim m^2$$

if $R_0 \sim 4m$ $\quad D_{turb} \sim 1\ m^2/sec$

$q \sim 3 \quad \alpha \sim 0.5 \quad C_s \sim 10^5\ m/sec$

then $\lambda_n^2 = \frac{1 \cdot 3 \cdot 4}{(0.5)\, 10^5} \sim 20 \cdot 10^{-5}$

$\sim 2\, 10^{-4}\ m^2$

$\lambda_n \sim 1.4\ 10^{-2} m \sim \mathcal{O}(cm)$!

Temp Profile Slightly Different:

$$\vec{\nabla} \cdot \vec{q}_{e,i} = \underbrace{Q_{e,i}}_{0 \text{ in SOL}} - \underbrace{P_{rad\, i,e}}_{0 \text{ for Simplicity}}$$

$$q_{r_{i,e}} \sim -n \chi^{turb}_{i,e} \nabla_r T_{i,e}$$

$$q_{\parallel_{i,e}} \sim -n \chi_\parallel \nabla_\parallel T_{i,e}$$

$\chi_\parallel \sim$ Spitzer Classical Collision Resistivity $\chi_\parallel \gg \chi^{turb}_{i,e}$

if $T \sim T_0 e^{-r/\lambda_T}$ then

$$-n\chi_{i,e}^{turb}\frac{T}{\lambda_T^2} \simeq -\frac{n\chi_{\parallel}T}{qR_0}$$

Solve for λ_T^2:

$$\lambda_T^2 \simeq \frac{qR_0\chi_{i,e}^{turb}}{\chi_{\parallel}}$$

$q \sim 3 \quad R_0 \sim 4m \quad \chi_{i,e}^{turb} \sim 1\ m^2/s$

$\chi_{\parallel} \sim$ Spitzer

$$\lambda_T \sim \mathcal{O}(cm)$$

if Power flux to target, $P \propto nT$

then $\dfrac{1}{\lambda_p} \simeq \dfrac{1}{\lambda_n} + \dfrac{1}{\lambda_T}$

$$\lambda_p \sim \frac{\lambda_n \lambda_T}{\lambda_n + \lambda_T} \lesssim \underline{\underline{1\,\mathrm{cm}}}$$

let us now estimate heat flux just outside LCFS in a hypothesized fusion reactor ...

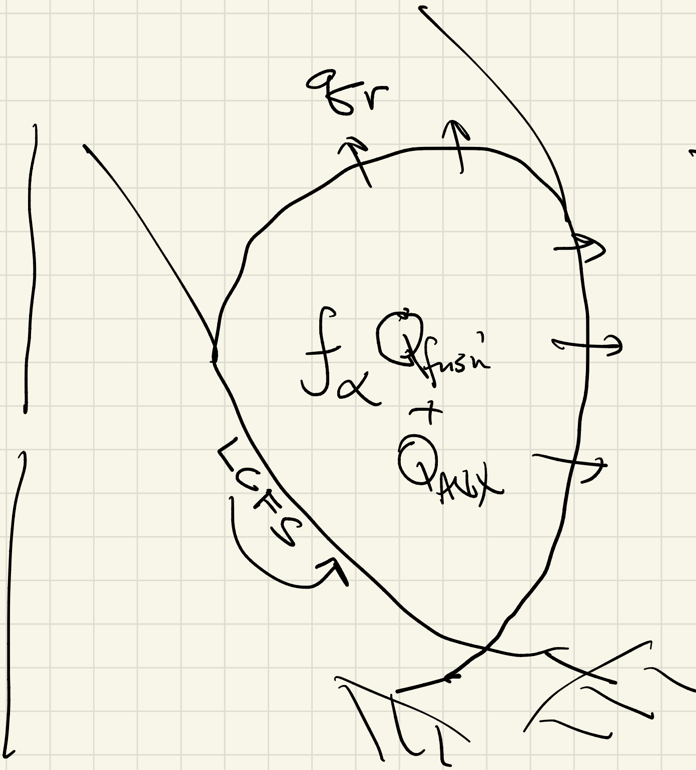

$f_\alpha = 0.2$

fraction of fusion energy into α particles

heat balance across LCFS

$$f_\alpha Q_{fusion} + \cancel{Q_{AUX}} = q_r S_{LCFS}$$

Ignited

LCFS Surface Area

Assume Perfect α confinement + thermalization

Assume Uniform

Now $S_{LCFS} \sim 2\pi R_0 \, 2\pi a \, K$

elongation

thus

$$f_\alpha Q_{fusion} = q_{\sigma r} \, 4\pi^2 R_0 a K$$

or $$q_{\sigma r} = \frac{f_\alpha Q_{fusion}}{4\pi^2 R_0 a K}$$

$R \sim 4m \quad a \sim 1m \quad K \sim 2$

$f_\alpha = 0.2 \quad Q_{fusion} \sim 500 \, MW$

$$q_{\sigma r}^{LCFS} \sim \frac{0.2 \; 500 \; 10^6}{40 \cdot 4 \cdot 2} \sim \frac{10^8}{300}$$

$$\sim 3 \, 10^5 \, W/m^2$$

Now what is $q_{\parallel}^{LCFS}$? From above it seems that...

$$q_{\parallel} \sim q_{\parallel}^{LCFS} \, e^{-r/\lambda_p}$$

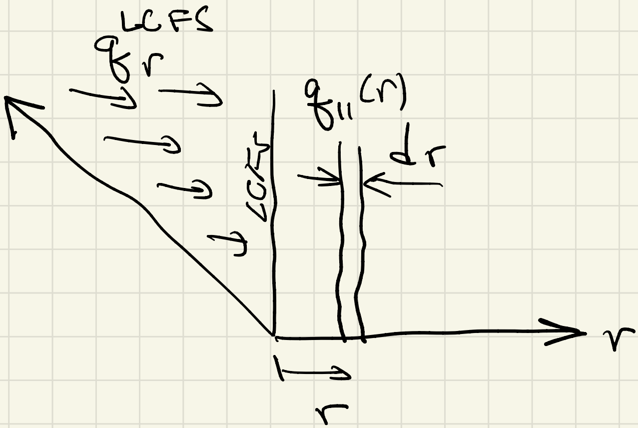

assuming $q_{\parallel}$ uniform w.r.t. θ

$$\int_{S_{LCFS}} \bar{q}_r \cdot d\underline{s} = \int_{r=r_{LCFS}=0}^{\infty} q_{\parallel}(r) \, dr \cdot \underbrace{2\pi a K}$$

$$f_\alpha Q_{fus} = q_{\parallel}^{LCFS} \int_{r=0}^{\infty} e^{-r/\lambda_p} \, dr \cdot 2\pi a K$$

$$f_\alpha Q_{fus} = 2\pi a K \, q_{\parallel}^{LCFS} \lambda_p$$

thus $q_{\parallel}^{LCFS} \simeq \dfrac{f_\alpha Q_{fus}}{2\pi a \kappa \lambda_p}$

$$\lambda_p = \frac{\lambda_n \lambda_T}{\lambda_n + \lambda_T} \sim 0.5 \text{ cm}$$

$$q_{\parallel}^{LCFS} \simeq \frac{0.2 \; 500 \; 10^6}{6 \cdot 1 \cdot 2 \cdot 5 \, 10^{-3}}$$

$$\simeq \frac{10^8}{6 \, 10^{-2}} \simeq 1.6 \, 10^9 \frac{W}{m^2}$$

(!!)

N.B. Re-entry from Earth orbit ~ 3 MW/m^2

Cutting Torch
Arc Welder $\}$: 10–100 MW/m^2

Clearly Must Reduce this heat flux!

How?

a) Expand Flux Surfaces in SOL before getting to target

b) Distribute heat over larger area via

i) radiation & recombination [dissipative divertor]

ii) Increase R_0, & which increase λ_n, λ_T & λ_p

[Super-X Divertor
Snowflake Divertor
Negative Tri Angularity

2. PMI: effect of materials on the plasma

→ a. Open Field Line Zone - S.O.L.

b. Plasma Sheaths

c. Impurities & Neutral Gas

Schematic View:

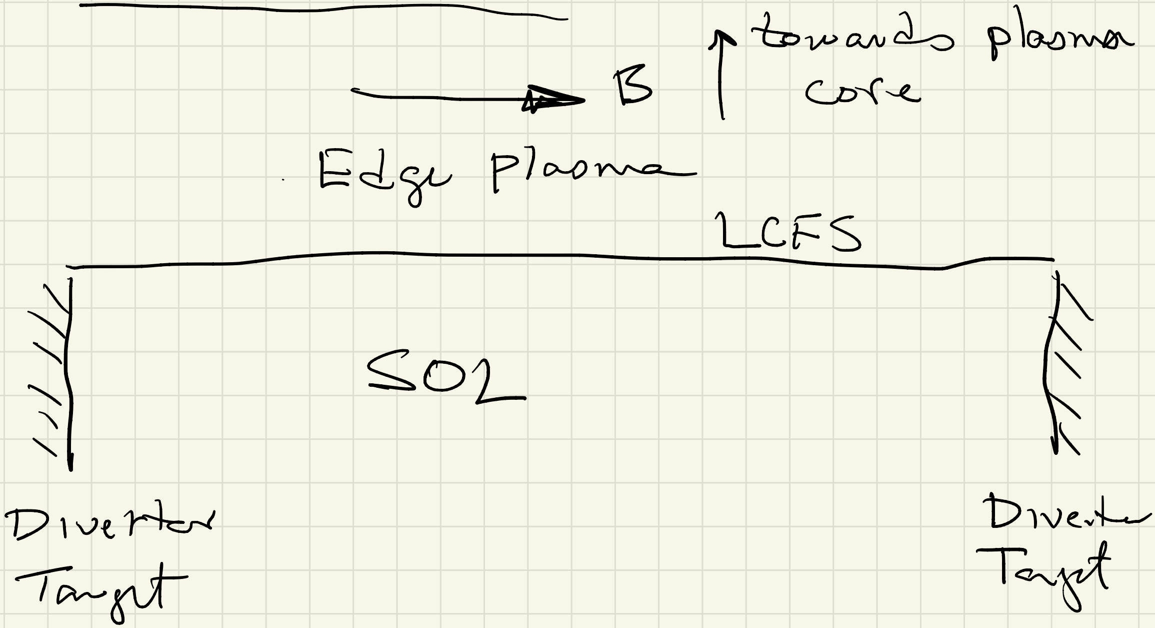

2. PMI: effect of materials on the plasma

a. Open Field Line Zone - S.O.L.

b. Plasma Sheaths

c. Impurities & Neutral Gas

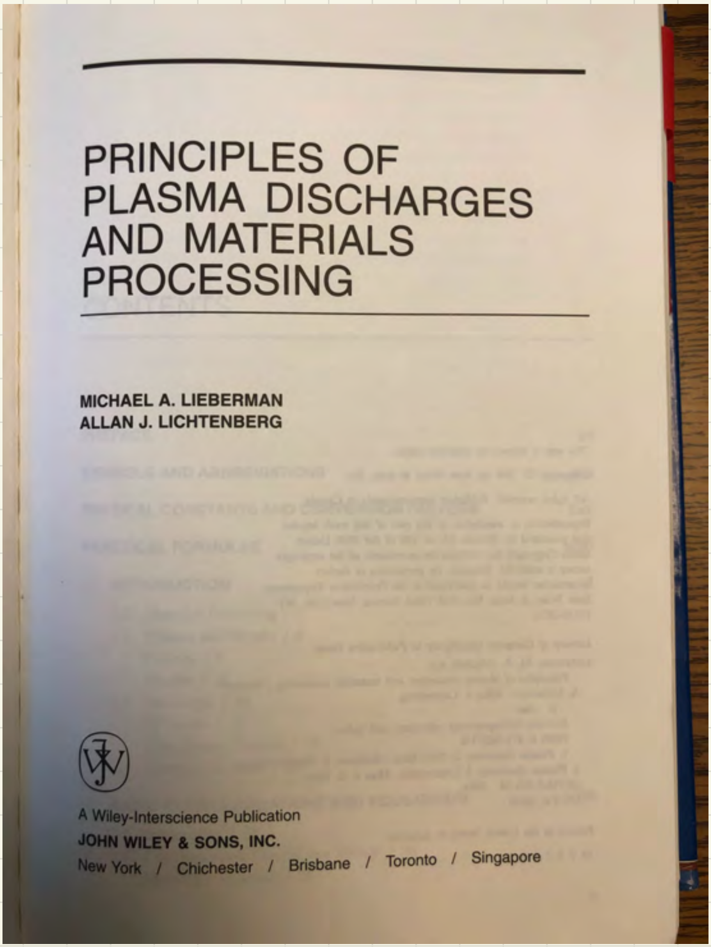

PRINCIPLES OF PLASMA DISCHARGES AND MATERIALS PROCESSING

MICHAEL A. LIEBERMAN
ALLAN J. LICHTENBERG

A Wiley-Interscience Publication
JOHN WILEY & SONS, INC.
New York / Chichester / Brisbane / Toronto / Singapore

CHAPTER 6

DC SHEATHS

6.1 BASIC CONCEPTS AND EQUATIONS

At the edge of a bounded plasma a potential exists to contain the more mobile charged species. This allows the flow of positive and negative carriers to the wall to be balanced. In the usual situation of an electropositive plasma, consisting of equal numbers of positive ions and electrons, the electrons are far more mobile than the ions. The plasma will therefore charge positively with respect to a grounded wall. The nonneutral potential region between the plasma and the wall is called a *sheath*.

In a weakly ionized plasma the energy to sustain the plasma is generally heating of the electrons by the source, while the ions are at near equilibrium with the background gas. The electron temperature is then typically of few volts, while the ions are cold. In this situation we may think of monoenergetic ions being accelerated through the sheath potential, while the electron density decreases according to a Boltzmann factor, as described in Section 2.4. The electron density would then decay on the order of a Debye length λ_{De}, to shield the electrons from the wall. However, we cannot linearize the Poisson equation, as we did in deriving λ_{De} in Section 2.4, if we wish to obtain the exact flux balance. Furthermore, we will show that a transition layer or *presheath* must exist between the neutral plasma and the nonneutral sheath in order to maintain the continuity of ion flux, giving rise to an ion velocity at the plasma-sheath edge known as the *Bohm velocity* u_B. The need for this presheath will arise naturally in our derivation in Section 6.2.

If a potential is placed between bounding electrodes, then, while the overall flux balance is maintained, each electrode may separately draw current. The most straightforward analysis is of a boundary with a large negative potential with respect to the plasma. The simplest example is a uniform ion charge density, or *matrix sheath*. This occurs in the cathode sheath of a dc discharge, for example, considered in Section 14.3. A matrix sheath is also created transiently with a pulsed negative electrode voltage in which the electrons are expelled from a plasma region, leaving a uniform ion density behind. This occurs naturally in *plasma immersion ion implantation*, discussed in Chapter 16. We consider the matrix sheath in Section 6.3.

For a high-voltage sheath, the current to the electrode is almost all ion current. Provided the ion motion in the sheath is collisionless, then the steady self-consistent ion density is not uniform, but rather is described by the *Child-Langmuir law of space-charge-limited current* in a planar diode. We also discuss this situation in Section 6.3.

The idealized conditions described in Sections 6.2 and 6.3 are not always met. The temperature of the ions cannot always be ignored with respect to the electron temperature. This situation arises, for example, in highly ionized plasmas. In this case more complicated kinetic treatments are required. In a similar vein, the electron distribution may not be Maxwellian. This may arise due to particular heating or loss mechanisms, which occur, for example, in low-pressure capacitive rf plasmas, discussed in Chapter 11. In this situation the decrease in electron density in the sheath is not given by a Boltzmann factor but must be obtained kinetically. If the neutral gas is electronegative, such that electron attachment is significant, then the negative charges divide between electrons and negative ions. If the fraction of negative ions present becomes large, the mobility of the negative charges can be greatly reduced, changing the conditions at the sheath edge. We consider these various topics, which, in fact, have some unity of analysis, in Section 6.4. Electronegative plasmas are of considerable importance in processing applications, and their analysis is described in Chapter 10.

Other situations that differ from the basic theory arise due to collisional effects in the sheath region. In this case the ion flow is impeded by collisional processes with neutrals, and the transport is mobility rather than inertia limited, similar to that already described in Chapter 5. We discuss two simple limiting collisional cases in Section 6.5. A full treatment, including both inertial and collisional effects, is very complicated, requiring numerical solution of the kinetic equations.

This chapter deals with sheaths that are constant in time. Two other interesting cases are sheaths formed in oscillating rf potentials and sheaths formed transiently by pulsed potentials. In both situations approximate solutions can be obtained if there is a separation of time scales such that electrons respond rapidly to the time variation while ions respond slowly. This separation is characterized by the inequalities

$$f_{pe} \gg \frac{1}{\tau} \gg f_{pi} \tag{6.1.1}$$

where τ is the time scale of field variation ($\tau = 2\pi/\omega$ for an oscillatory variation) and f_{pe} and f_{pi} are the electron and ion plasma frequencies, respectively. An oscillatory potential applied to an electrode is characteristic of a capacitively excited rf discharge, and we consider this sheath in Chapter 11. The pulsed potential sheath is analyzed in Chapter 16.

The Collisionless Sheath

We use the assumptions (1) Maxwellian electrons at temperature T_e, (2) cold ions ($T_i = 0$), and (3) $n_e(0) = n_i(0)$ at the plasma–sheath interface (interface between essentially neutral and nonneutral regions) at $x = 0$. As shown in Fig. 6.1, we define the zero of the potential Φ at $x = 0$ and take the ions to have a velocity u_s there. Ion energy conservation (no collisions) then gives

$$\frac{1}{2}Mu^2(x) = \frac{1}{2}Mu_s^2 - e\Phi(x) \tag{6.1.2}$$

The continuity of ion flux (no ionization in the sheath) is

$$n_i(x)u(x) = n_{is}u_s \tag{6.1.3}$$

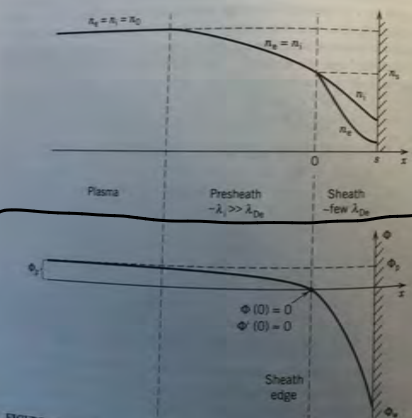

FIGURE 6.1. Qualitative behavior of sheath and presheath in contact with a wall.

where n_{is} is the ion density at the sheath edge. Solving for u from (6.1.2) and substituting in (6.1.3) we have

$$n_i = n_{is}\left(1 - \frac{2e\Phi}{Mu_s^2}\right)^{-1/2} \tag{6.1.4}$$

The electron density is given by the Boltzmann relation

$$n_e(x) = n_{es}e^{\Phi(x)/T_e} \tag{6.1.5}$$

Setting $n_{es} = n_{is} \equiv n_s$ at the sheath edge and substituting n_i and n_e into Poisson's equation

$$\frac{d^2\Phi}{dx^2} = \frac{e}{\epsilon_0}(n_e - n_i)$$

we obtain

$$\boxed{\frac{d^2\Phi}{dx^2} = \frac{en_s}{\epsilon_0}\left[\exp\frac{\Phi}{T_e} - \left(1 - \frac{\Phi}{\mathcal{E}_s}\right)^{-1/2}\right]} \tag{6.1.6}$$

where $e\mathcal{E}_s = \frac{1}{2}Mu_s^2$ is the initial ion energy. Equation (6.1.6) is the basic nonlinear equation governing the sheath potential and ion and electron densities. However, as we shall see in the next section, it has stable solutions only for sufficiently large u_s, created in an essentially neutral *presheath* region.

6.2 THE BOHM SHEATH CRITERION

A first integral of (6.1.6) can be obtained by multiplying (6.1.6) by $d\Phi/dx$ and integrating over x:

$$\int_0^{\Phi}\frac{d\Phi}{dx}\frac{d}{dx}\left(\frac{d\Phi}{dx}\right)dx = \frac{en_s}{\epsilon_0}\int_0^{\Phi}\frac{d\Phi}{dx}\left[\exp\frac{\Phi}{T_e} - \left(1 - \frac{\Phi}{\mathcal{E}_s}\right)^{-1/2}\right]dx \tag{6.2.1}$$

Canceling the dx's and integrating with respect to Φ, we obtain

$$\frac{1}{2}\left(\frac{d\Phi}{dx}\right)^2 = \frac{en_s}{\epsilon_0}\left[T_e\exp\frac{\Phi}{T_e} - T_e + 2\mathcal{E}_s\left(1 - \frac{\Phi}{\mathcal{E}_s}\right)^{1/2} - 2\mathcal{E}_s\right] \tag{6.2.2}$$

where we have set $\Phi = 0$ and $d\Phi/dx = 0$ at $x = 0$ corresponding to a field free plasma. Equation (6.2.2) can be integrated numerically to obtain $\Phi(x)$. However, it is apparent that the RHS of (6.2.2) should be positive for a solution to exist. Physically this means that the electron density must always be less than the ion density in the sheath region. Since we expect this to be a problem only for small Φ, we expand the RHS of (6.2.2) to second order in a Taylor series to obtain the inequality

$$\frac{1}{2}\frac{\Phi^2}{\mathrm{T_e}} - \frac{1}{4}\frac{\Phi^2}{\mathcal{E}_s} \geq 0 \tag{6.2.3}$$

We see that (6.2.3) is satisfied for $\mathcal{E}_s \geq \mathrm{T_e}/2$ or, substituting for $\mathcal{E}_s$,

$$u_s \geq u_B = \left(\frac{e\mathrm{T_e}}{M}\right)^{1/2} \tag{6.2.4}$$

This result is known as the *Bohm sheath criterion*. To give the ions this directed velocity u_s, there must be a finite electric field in the plasma over some region, typically much wider than the sheath, called the *presheath* (see Fig. 6.1). Hence the presheath region is not strictly field free, although E is very small there. Since the field at the edge between the sheath and the presheath is not precisely defined, only approximate solutions are obtained by matching sheath to presheath solutions. Nevertheless, if we can make (6.2.4) sharper, by using the equality on the right, this relation is sufficient to obtain quantitative solutions for the plasma equilibrium. The procedure for doing this is to examine the solution in the presheath region of the plasma in the quasineutral approximation $n_i = n_e$, to see how the presheath solution joins with that of the sheath region. We sketch the calculation below.

Presheath Requirements

Setting

$$n_i = n_e \tag{6.2.5}$$

within the presheath and taking the derivative of the logarithm of (6.2.5) we have

$$\frac{1}{n_i}\frac{\mathrm{d}n_i}{\mathrm{d}x} = \frac{1}{n_e}\frac{\mathrm{d}n_e}{\mathrm{d}x} \tag{6.2.6}$$

Substituting on the left for the ion current, through the relation $n_i = J_i/eu_i$, this becomes

$$\frac{1}{J_i}\frac{\mathrm{d}J_i}{\mathrm{d}x} - \frac{1}{u_i}\frac{\mathrm{d}u_i}{\mathrm{d}x} = \frac{1}{n_e}\frac{\mathrm{d}n_e}{\mathrm{d}x} \tag{6.2.7}$$

Assuming the Boltzmann form of n_e and rearranging, (6.2.7) becomes

$$\frac{1}{u_i}\frac{\mathrm{d}u_i}{\mathrm{d}x} + \frac{1}{\mathrm{T_e}}\frac{\mathrm{d}\Phi}{\mathrm{d}x} = \frac{1}{J_i}\frac{\mathrm{d}J_i}{\mathrm{d}x} \tag{6.2.8}$$

In the presheath we expect the flow to be subsonic, with $u_i < u_B$, and applying this condition to (6.2.8) we have

$$\frac{1}{u_B}\frac{\mathrm{d}u_i}{\mathrm{d}x} + \frac{1}{\mathrm{T_e}}\frac{\mathrm{d}\Phi}{\mathrm{d}x} < \frac{1}{J_i}\frac{\mathrm{d}J_i}{\mathrm{d}x} \tag{6.2.9}$$

This is satisfied for either

$$\frac{1}{u_B}\frac{\mathrm{d}u_i}{\mathrm{d}x} + \frac{1}{\mathrm{T_e}}\frac{\mathrm{d}\Phi}{\mathrm{d}x} < 0, \qquad \frac{1}{J_i}\frac{\mathrm{d}J_i}{\mathrm{d}x} = 0 \tag{6.2.10}$$

or

$$\frac{1}{u_B}\frac{\mathrm{d}u_i}{\mathrm{d}x} + \frac{1}{\mathrm{T_e}}\frac{\mathrm{d}\Phi}{\mathrm{d}x} > 0, \qquad \frac{1}{J_i}\frac{\mathrm{d}J_i}{\mathrm{d}x} > \frac{1}{u_B}\frac{\mathrm{d}u_i}{\mathrm{d}x} + \frac{1}{\mathrm{T_e}}\frac{\mathrm{d}\Phi}{\mathrm{d}x} \tag{6.2.11}$$

Since the ion energy conservation (6.1.2) would make

$$\frac{1}{u_B}\frac{\mathrm{d}u_i}{\mathrm{d}x} + \frac{1}{\mathrm{T_e}}\frac{\mathrm{d}\Phi}{\mathrm{d}x} > 0$$

relations (6.2.10) imply ion friction in the presheath, whereas taking the equality on the right implies current conservation. Relations (6.2.11) imply ionization or geometric contraction. At the sheath–presheath interface there is a transition from subsonic to supersonic ion flow, where the condition of charge neutrality must break down. Putting in specific values of momentum mean free path, ionization, or geometric contraction, the presheath equations can be solved analytically. This has been done, for example, for (a) a geometric presheath with current contraction onto a spherical probe, (b) a plane parallel collisional presheath, and (c) an ionizing presheath with the ionization proportional to n_e. These solutions are plotted in Fig. 6.2. They show quite different behavior in the plasma region: The geometric presheath (a) relaxes to the undisturbed (field free) plasma, the collisional presheath (b) tends to a logarithmic potential shape (indicating that the ion transport requires a residual plasma field), and the ionizing presheath (c) ends with zero field at a finite point representing the midplane of a symmetric plasma. For (b) or (c) the presheath width is of order the mean free path for ion-neutral collisions or for electron-neutral ionization, respectively. Despite the differences, all solutions run quite similarly into the singularity $u_i = u_B$ at the sheath edge. The growing field inhomogeneity approaching this singularity indicates the formation of space charge and the breakdown of the quasineutral approximation. Matching the ion velocity across the sheath–presheath interface then gives us the equality $u_i = u_B$ for the sheath region. Of course, the true behavior is quite complicated at this interface, thus needing a more sophisticated treatment. For more details, including a kinetic treatment, the reader is referred to a review paper by Riemann (1991).

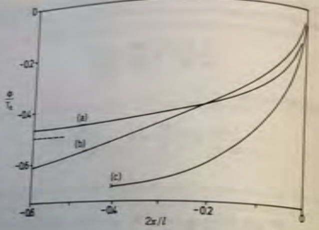

FIGURE 6.2. Φ/T_e versus position within the presheath, showing (a) the geometric presheath, (b) a planar collisional presheath, and (c) a planar ionization presheath. The sheath–presheath edge is at the right (after Riemann, 1991).

The potential drop across the presheath, which accelerates the ions to the Bohm velocity, is given by

$$\frac{1}{2}Mu_B^2 = e\Phi_p$$

where Φ_p is the plasma potential with respect to the potential at the sheath–presheath edge. Substituting for the Bohm velocity from (6.2.4), we find

Presheath $\Delta\Phi$

$$\boxed{\Phi_p = \frac{\mathrm{T}_e}{2}} \tag{6.2.12}$$

This is shown as the dashed line in Fig. 6.1. The ratio of the density at the sheath edge to that in the plasma is then found from the Boltzmann relation

$$n_s = n_b e^{-\Phi_p/\mathrm{T}_e} \approx 0.61 n_b \tag{6.2.13}$$

where n_b is the density where the presheath and bulk plasma join.

Sheath Potential at a Floating Wall

It is quite straightforward to determine the potential drop within the sheath between a plasma and a floating wall. We equate the ion flux (assumed constant through the sheath),

$$\Gamma_i = n_s u_B \tag{6.2.14}$$

to the electron flux at the wall,

$$\Gamma_e = \frac{1}{4} n_s \bar{v}_e e^{\Phi_w/\mathrm{T}_e} \tag{6.2.15}$$

where $\bar{v}_e = (8e\mathrm{T}_e/\pi m)^{1/2}$ is the mean electron speed and Φ_w is the potential of the wall with respect to the sheath–presheath edge. We have, after substituting for the Bohm velocity from (6.2.4),

$$n_s\left(\frac{e\mathrm{T}_e}{M}\right)^{1/2} = \frac{1}{4}n_s\left(\frac{8e\mathrm{T}_e}{\pi m}\right)^{1/2} e^{\Phi_w/\mathrm{T}_e} \tag{6.2.16}$$

Solving for Φ_w, we obtain

$$\Phi_w = -\mathrm{T}_e \ln\left(\frac{M}{2\pi m}\right)^{1/2} \tag{6.2.17}$$

The wall potential Φ_w is negative and is related linearly to T_e with a factor proportional to the logarithm of the square root of the mass ratio. For hydrogen, for example, $\ln(M/2\pi m)^{1/2} \approx 2.8$, while for argon ($M = 40$ amu) the factor is 4.7. Thus argon ions with initial energy $\mathcal{E}_s = \mathrm{T}_e/2$ at the sheath–presheath edge that fall through a collisionless dc sheath to a floating wall would bombard the wall with an energy of $\mathcal{E}_i \approx 5.2\mathrm{T}_e$. Of course, electrodes that have potentials on them, either dc or rf, can be bombarded with much higher energy, but these electrodes must draw a substantial net current, as we will show in Section 6.3.

The sheath width s is found by integrating (6.2.2) to obtain $\Phi(x)$ and setting $\Phi(s) = \Phi_w$, with Φ_w given by (6.2.17). The integral must be done numerically. Typical sheath widths are a few electron Debye lengths λ_{De}.

Particle-in-cell simulations can illustrate some of the phenomena we have described, as well as introduce some new features. Figure 6.3 shows a simulation of sheath formation during the decay of a warm, initially uniform density electron–proton plasma between short-circuited parallel plates (no source). The initial plasma parameters are $\mathrm{T}_e = \mathrm{T}_i = 1$ V and $n_0 = 10^8$ cm^{-3}, with $p = 50$ mTorr, $l = 1$ cm, and an ion-neutral momentum transfer cross section $\sigma_{mi} = 5 \times 10^{-15}$ cm^2. For these parameters, $\lambda_{De} \approx 0.074$ cm, $f_{pe}^{-1} \approx 1.11 \times 10^{-8}$ s, $D_a \approx 1.5 \times 10^5$ cm^2/s, and the fundamental diffusion mode timescale is $\tau_0 \approx 0.68 \times 10^{-6}$ s. The density, field, and potential profiles are shown in (a), (b), and (c) at $t = 5 \times 10^{-8}$ s, after the sheaths have partially formed, but before the decay of the higher-order ($i > 1$) diffusion modes. Hence the ion density in (a) is relatively uniform in the bulk plasma rather than the cosine variation given in (5.2.7), and the steady-state sheaths have not fully formed due to ion transit timescale effects. However, we clearly see the sheath formation. The midpotential variation with time is shown on a short timescale in (d), illustrating its formation with $\Phi_{max} \sim \mathrm{T}_e$ as the sheaths form on the very fast electron timescale f_{pe}^{-1}, along with accompanying electron plasma oscillations, as noted previously for Fig. 2.2.

Result from our lab, Nishijima RSI 2020

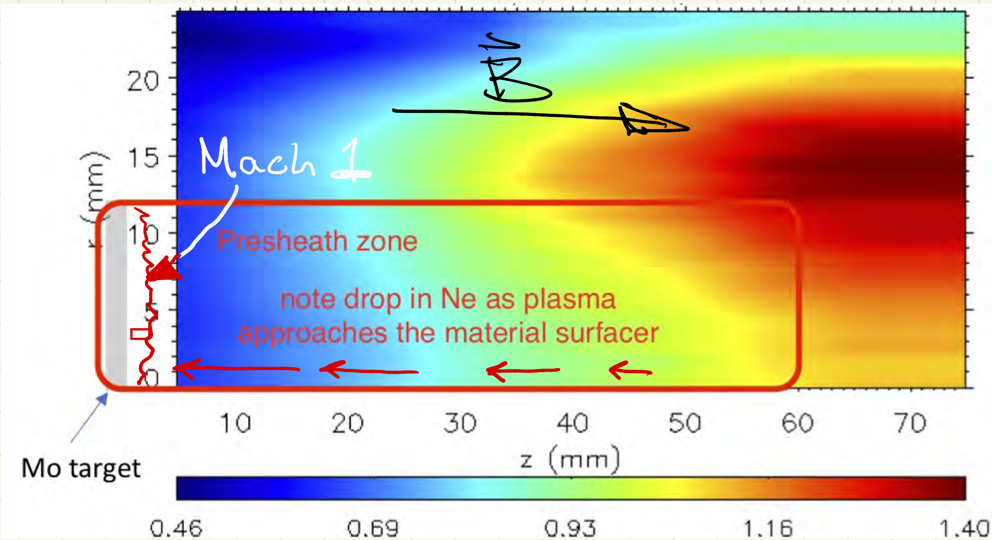

Note: $\nabla_{\parallel} n_e$ in pre-sheath zone; $\delta n_e \sim \frac{1}{2} n_e^{upstream}$

Since Boltzmann Relation holds along B...

$$n_e = n_{e_0} \exp(-e\phi/(kT_e))$$

$\Rightarrow$ $E_{\parallel}$ exists in presheath $\Rightarrow$ Flow

Implications of Sheaths;

1) $\overline{v}_{\parallel} \simeq C_s$ at sheath-presheath boundary

2) $\Delta\phi_{sheath} \simeq K\, T_e$; $K \sim 3$ for H plasmas

$\hookrightarrow$ Ions hit surface w/ few $\times\, T_e$ kinetic energy

3) Sheath Introduces a <u>New</u> <u>Dissipation</u> for $\parallel$ electron motion

4) Since $\Delta\phi_{sheath} = K\, T_e$ & $T_e = T_e(r)$

$\Longrightarrow \Delta\phi_{sheath} = \Delta\phi_{sh}(r)$

Take these two results up in reverse order:

Sheath Dissipation Effects

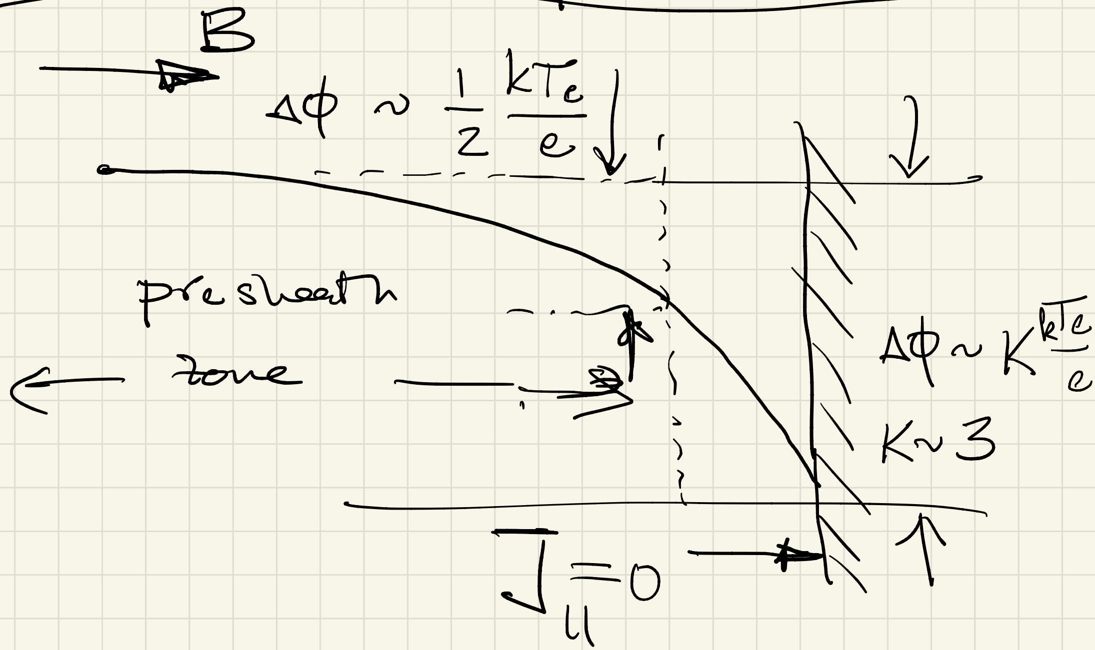

this balance gives $\langle J_{\parallel} \rangle = 0$

here $\langle \cdots \rangle \equiv \frac{1}{T}\int_0^T (\cdots)\,dt$

But... if $\phi = \overline{\phi} + \tilde{\phi}$

$$n = \overline{n} + \tilde{n}$$

fluctuation due to turbulence

Can show that $J_{\parallel e}$ at sheath edge satisfies

$$\nabla_\parallel J_\parallel = \frac{kT_e}{e\eta_\parallel} \nabla_\parallel^2 \left(\frac{e\tilde{\phi}}{kT_e} - \frac{\tilde{n}}{\overline{n}} \right)$$

[for small $\frac{e\tilde{\phi}}{kT}, \frac{\tilde{n}}{\overline{n}}$]

Key Take-Away:

plasma sheath introduces a new source of // e^- motion dissipation!

n.b. parallel dissipation is key to D.W. instability

Now begin to put picture of Edge/SOL plasma together:

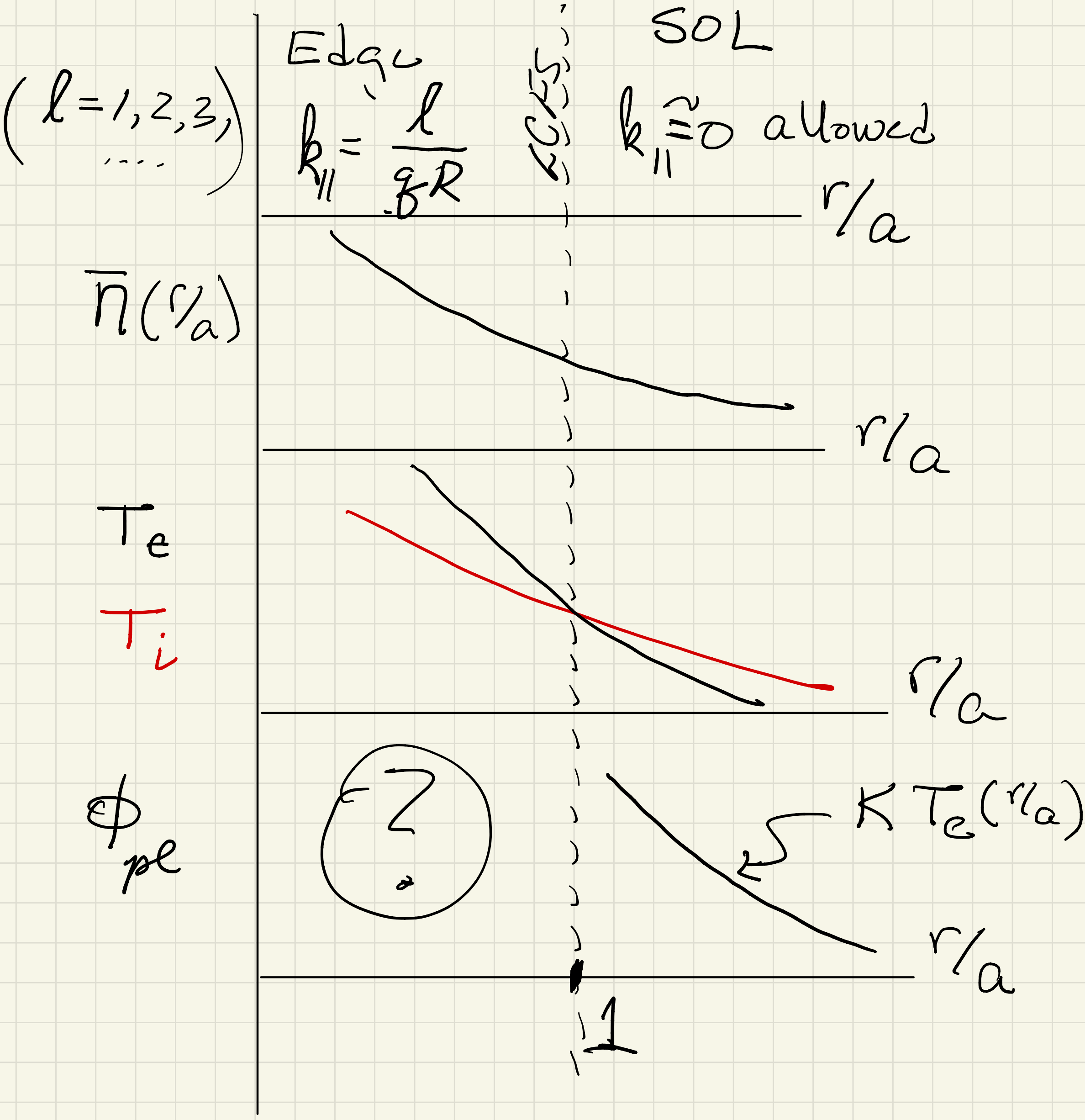

$\phi_{pl}(r/a)$ for $r/a < 1$?

look at $\hat{r}$ component of ion momentum:

$$m_i n \left(\cancel{\frac{\partial}{\partial t} + \vec{v} \cdot \nabla} \right) \bar{v}_r = qn E_r - \nabla p_i \cancel{\bar{v}_i \times \bar{B}} + \cdots$$

$\to 0$

small if strong damping

$$\boxed{\Rightarrow \; E_r = \frac{\nabla p_i}{qn} < 0 \quad \text{for } \frac{r}{a} < 1}$$

Now begin to put picture of Edge/SOL plasma together:

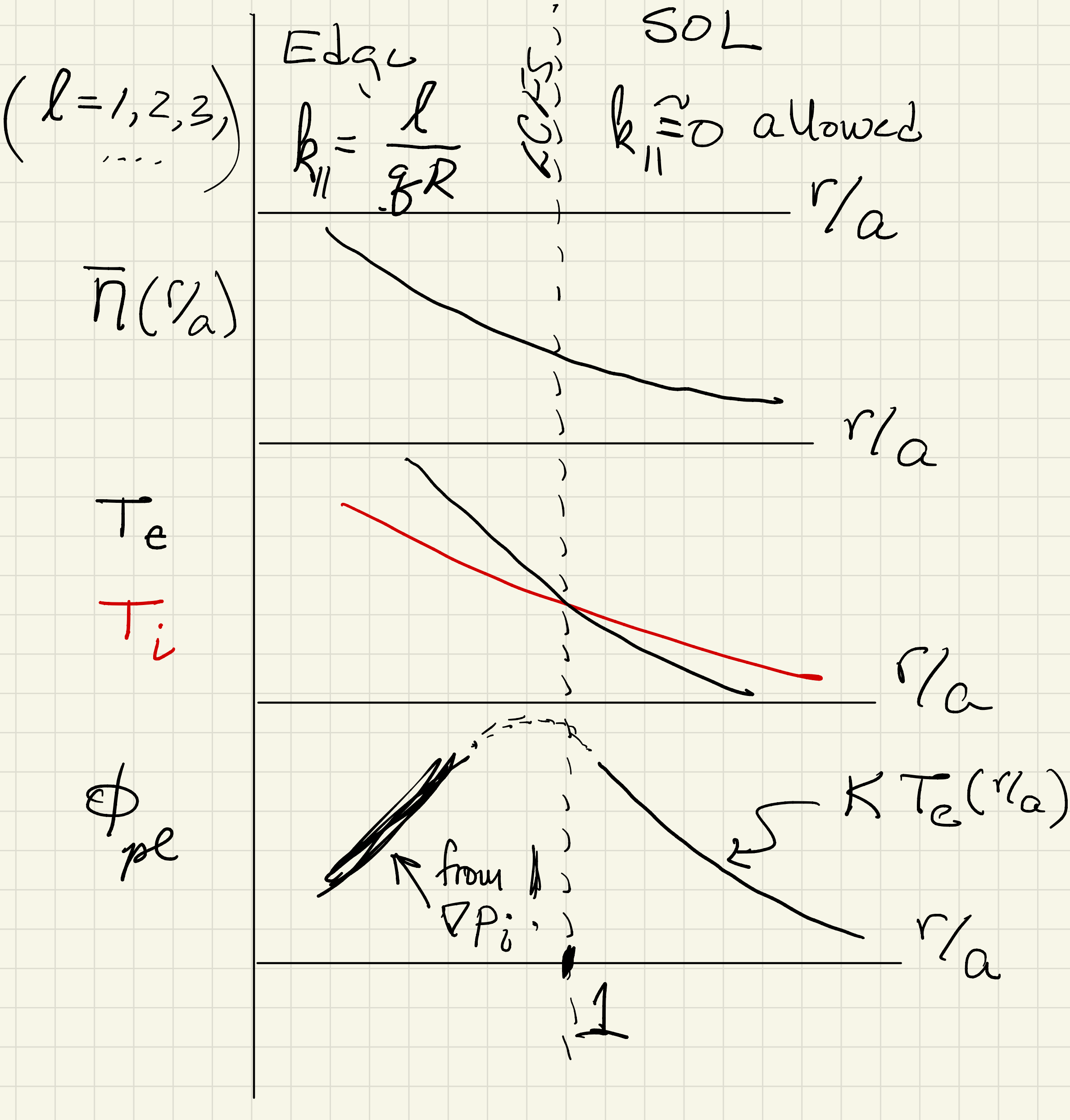

Now begin to put picture of Edge/SOL plasma together:

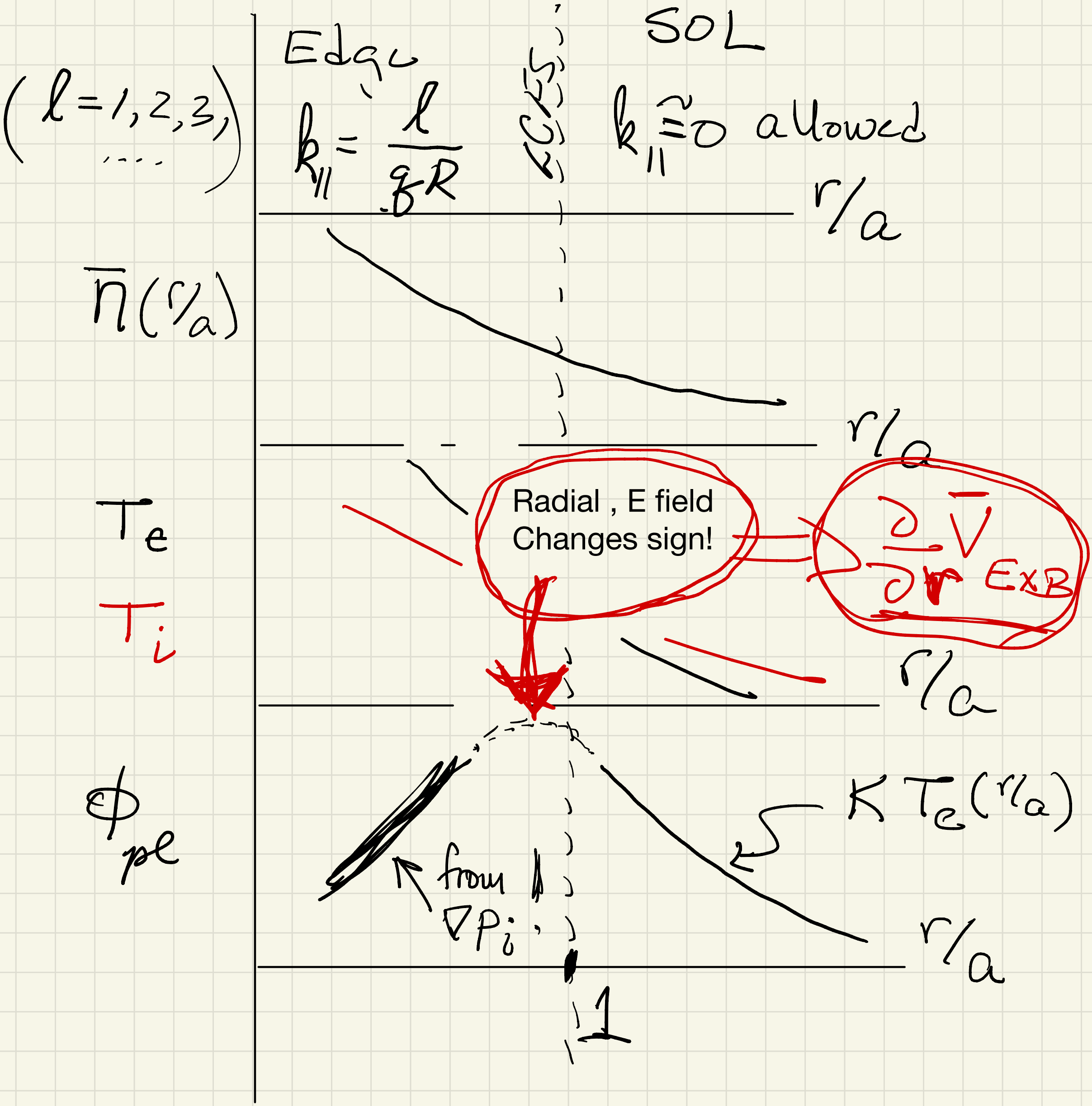

Now begin to put picture of Edge/SOL plasma together:

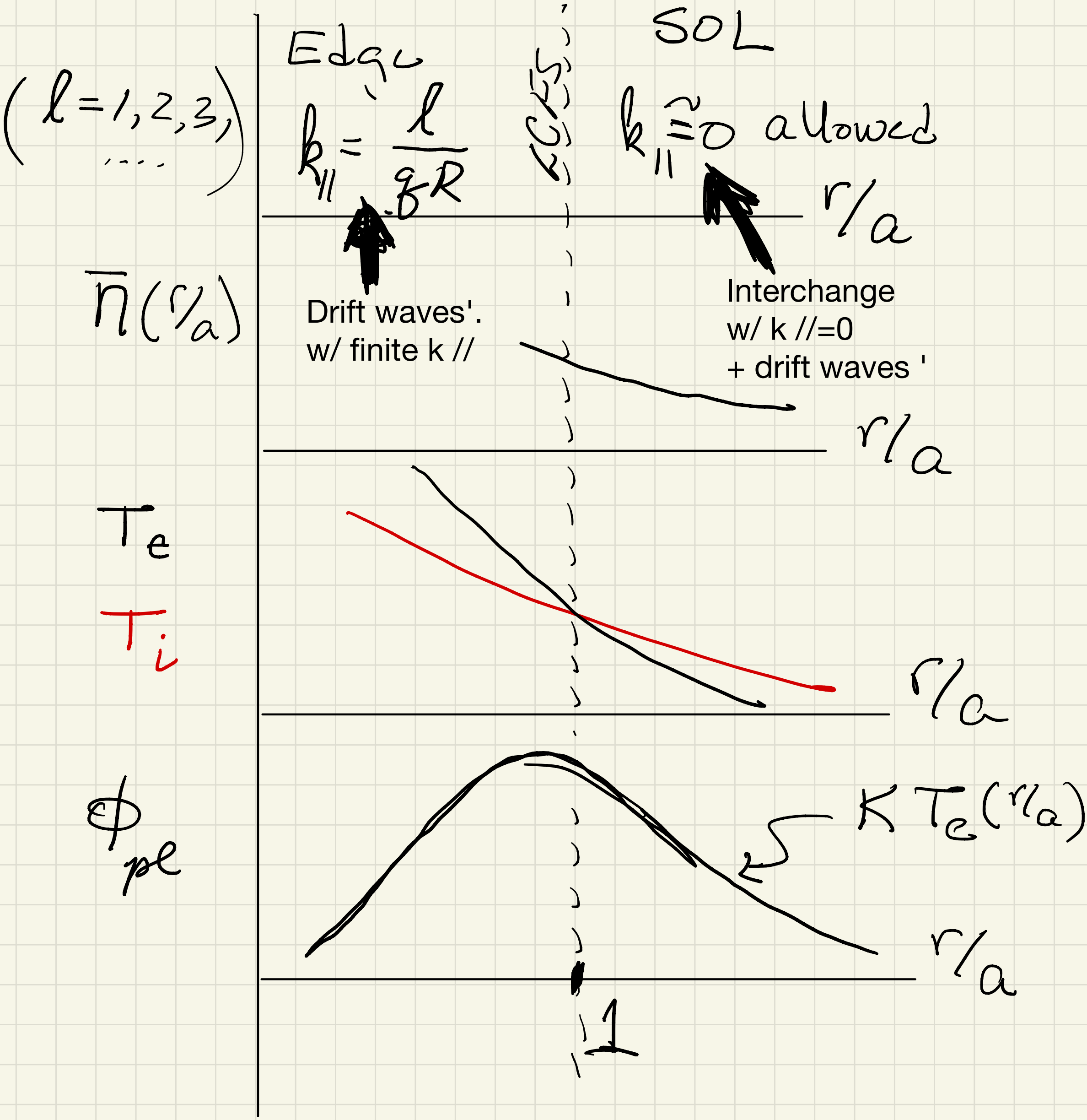

Key Results:

1) $\vec{E} \times \bar{B}_0$ shear naturally exists at LCFS

2) Drift-Turbulence ($|k_{\parallel}| > 0$) inside LCFS;

Drift-Turb. ⊕ Interchange ($k_{\parallel} \sim 0$) in SOL

3) Increased Heating will Increase $E \times B$ shear layer

4) Increased damping of $E \times B$ flow (ion-neutral CX, trapped-passing ion collisions, electron collisions)

$n/n_G \uparrow$

$\Downarrow$

$\left|\frac{\partial V_E}{\partial r}\right|_{LCFS}$ reduced

Key Results:

$\boxed{\text{1) } \vec{E} \times \bar{B}_0 \text{ shear naturally exists at LCFS}}$

2) Drift-Turbulence ($|k_{\parallel}| > 0$) inside LCFS;
Drift-Turb. ⊕ Interchange ($k_{\parallel} \sim 0$) in SOL

3) Increased Heating will Increase $E \times B$ shear layer

4) Increased damping of $E \times B$ flow (ion-neutral CX, trapped-passing ion collisions, electron collisions)

$$\left|\frac{\partial V_E}{\partial r}\right|_{LCFS} \cdot \text{reduced} \quad \cdot \quad n/n_G \uparrow$$

First evidence for $E \times B$ shear layer at LCFS

Ritz, Phy Fluids '84

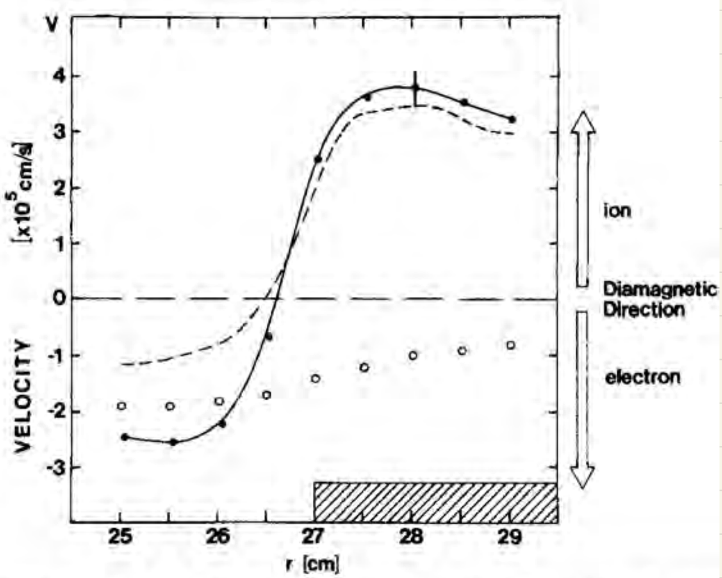

FIG. 3. Radial profile of measured phase velocity (—), $E_r \times B$ veloc (– – –), and gradient driven drift velocity $V_{\nabla p}$(○). The limiter position shown in the shaded area.

the transport is always outward. This is a result of t fa that both the wavenumber $\bar{k}(\omega)$ and phase angle α chan sign as the probes are moved radially

$$\frac{\partial V_{E\times B}}{\partial r} \Rightarrow$$ tilting of turbulent structures

azimuthally separated probe tips in order to estimate fluctuations in the azimuthal electric field E_θ. Figure 9(a) shows the radial profile of turbulent particle flux measured for four different bias voltages. The flux is computed using the fast

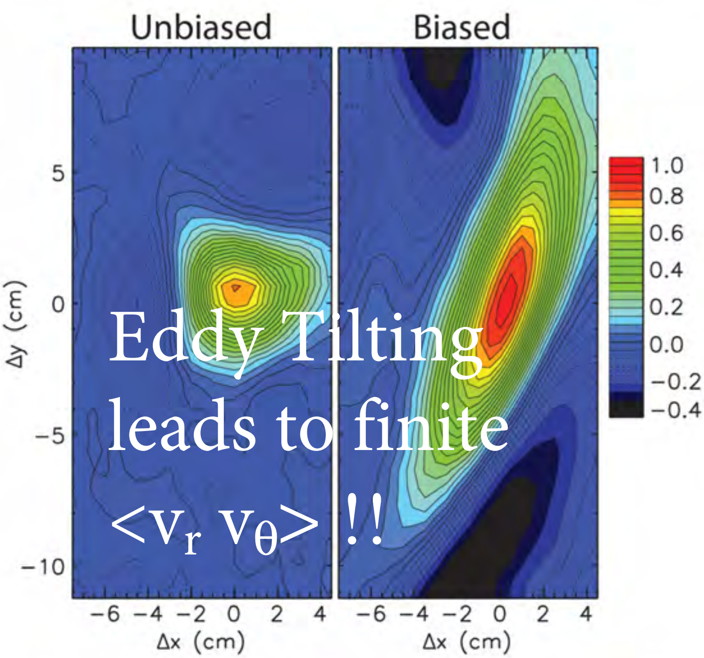

FIG. 8. (Color) Two-dimensional cross-field correlation function for I_{sat} fluctuations in unbiased and biased plasmas.

Key Results:

1) $\vec{E} \times \bar{B}_0$ shear naturally exists at LCFS

2) Drift-Turbulence ($|k_{\parallel}| > 0$) inside LCFS;
Drift-Turb. ⊕ Interchange ($k_{\parallel} \sim 0$) in SOL

3) Increased Heating will Increase $E \times B$ shear layer

4) Increased damping of $E \times B$ flow (ion-neutral CX, trapped-passing ion collisions, electron collisions)

$\Downarrow$

$\left|\frac{\partial V_E}{\partial r}\right|_{LCFS}$ reduced

$n/n_G \uparrow$

Bursty, Intermittent Turbulence in SOL

Zweben NF '04 NSTX

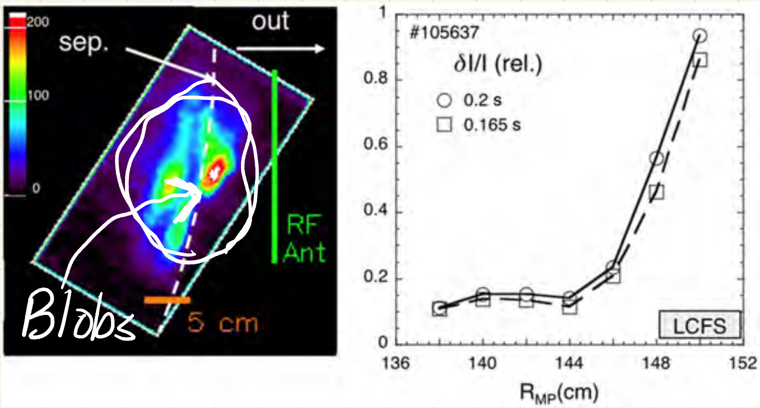

Boedo, PoP '01

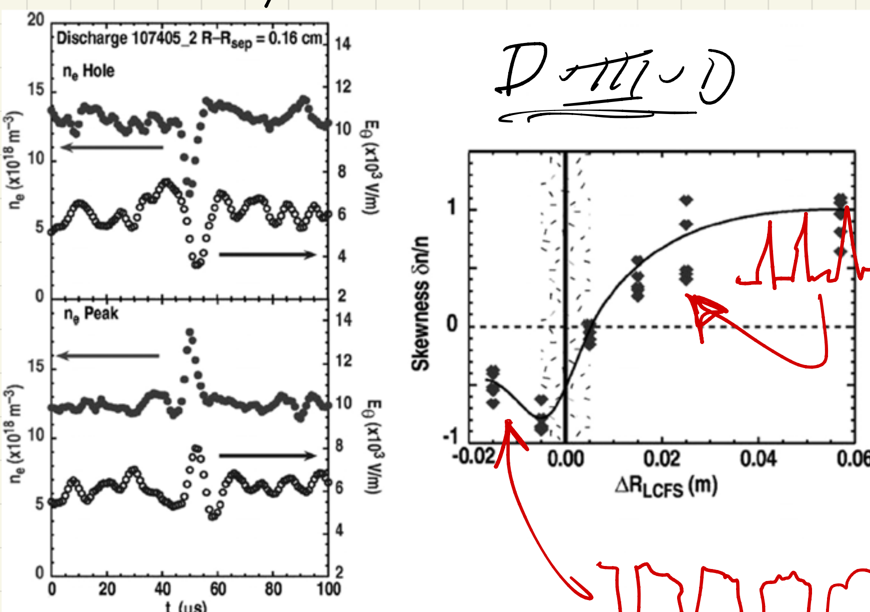

D-III-D

blobs

"holes"

C-Mod

Grulke PoP '06

dipolar potential

outgoing $\delta n > 0$ event

outgoing minor radius

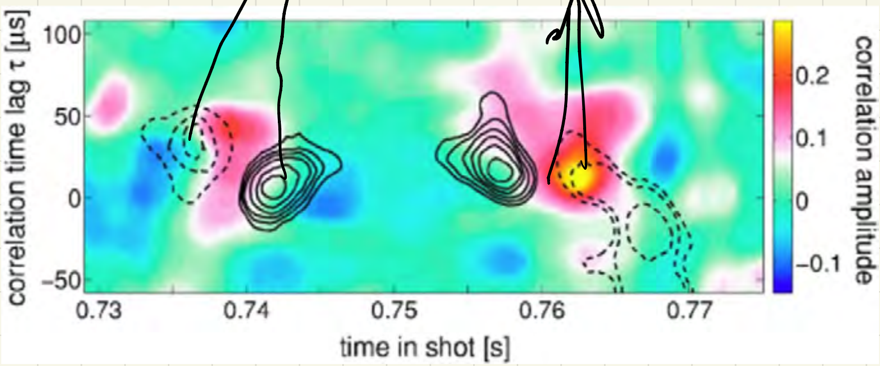

$\propto$ poloidal position

Key Results:

1) $\vec{E} \times \bar{B}_0$ shear naturally exists at LCFS

2) Drift-Turbulence ($|k_{\parallel}| > 0$) inside LCFS;
Drift-Turb. ⊕ Interchange ($k_{\parallel} \sim 0$) in SOL

3) Increased Heating will Increase $E \times B$ shear layer

4) Increased damping of $E \times B$ flow (ion-neutral CX, trapped-passing ion collisions, electron collisions)

$\Downarrow$

$\left|\frac{\partial V_E}{\partial r}\right|_{LCFS}$ reduced

$n/n_G \uparrow$

Increased P_{aux} leads to stronger ExB shear layer

Xu, PRL '12 HL-2A

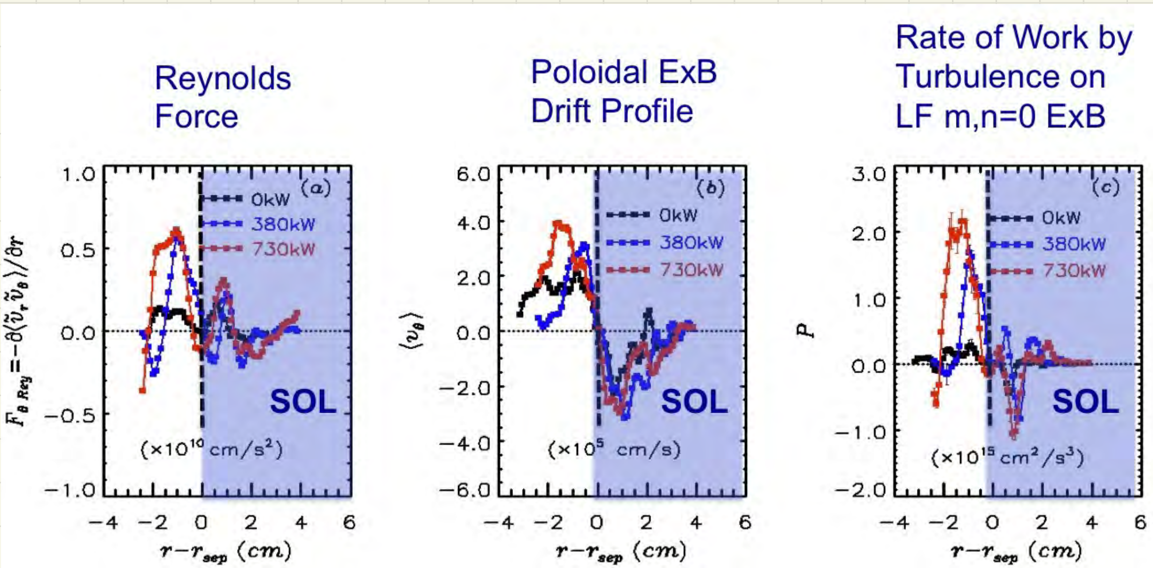

V_E'

Reynolds Force

Eddies Tilt

Key Results:

1) $\vec{E} \times \bar{B}_0$ shear naturally exists at LCFS

2) Drift-Turbulence ($|k_{\parallel}| > 0$) inside LCFS;
Drift-Turb. ⊕ Interchange ($k_{\parallel} \sim 0$) in SOL

3) Increased Heating will Increase $E \times B$ shear layer

4) Increased damping of $E \times B$ flow (ion-neutral CX, trapped-passing ion collisions, electron collisions)

$\Rightarrow \left| \frac{\partial V_E}{\partial r} \right|_{LCFS}$ reduced . $n/n_G \uparrow$

As $\frac{n}{n_G}\uparrow$, ExB shear & Reynolds Stress Weakens

Hong NF '18 HL-2A

3:50 PM Sat Jun 5 76%

Edge Trubulence and Shear Flows... 2018_Nucl._Fusion_58_016041 PDF

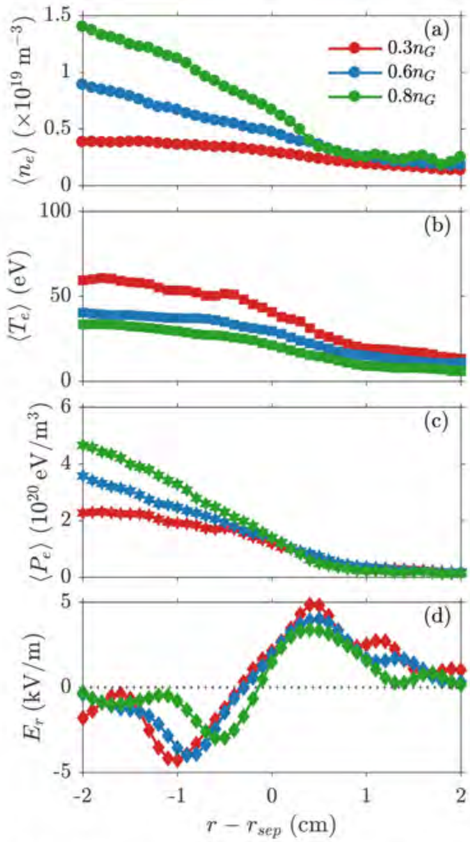

Figure 1. Equilibrium profiles of the electron density (*a*), electron temperature (*b*), el~~ectron pressure (*c*) and radial~~ electric field (*d*), at

Figure 2. turbulent $\mathcal{P}_{\mathrm{Re}} = -$ densities (EDD) di di...on.

At lower

... add turbulent fluxes into SOL increase, N. L. flowdrive dies

Hong NF'18 HL-2A

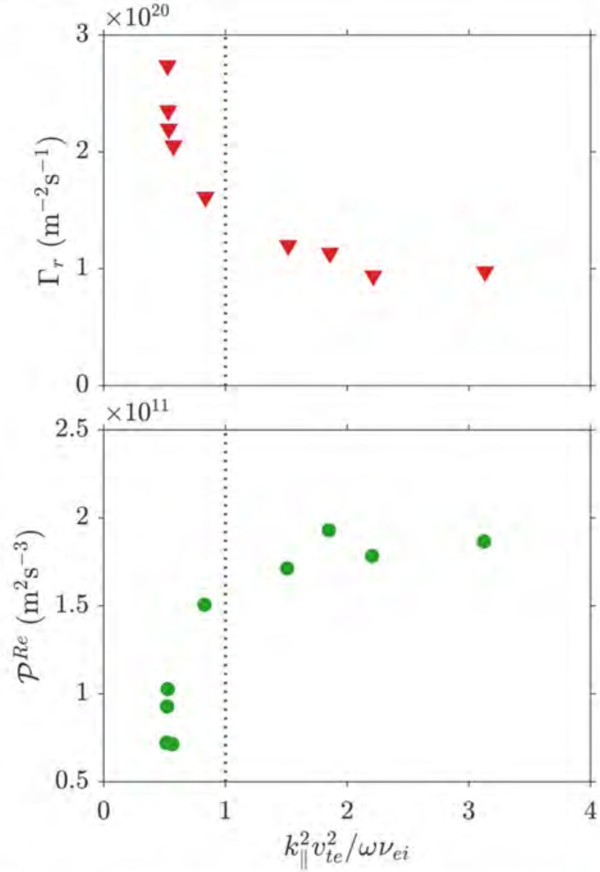

Figure 11. The volume averaged particle flux (upper) and Reynolds power (bottom) plotted as a function of the adiabatic parameter.

Global 3D two-fluid simulations of the tokamak edge region: Turbulence, transport, profile evolution, and spontaneous E × B rotation

Ben Zhu, Manaure Francisquez, and Barrett N. Rogers

Citation: Physics of Plasmas **24**, 055903 (2017); doi: 10.1063/1.4978885

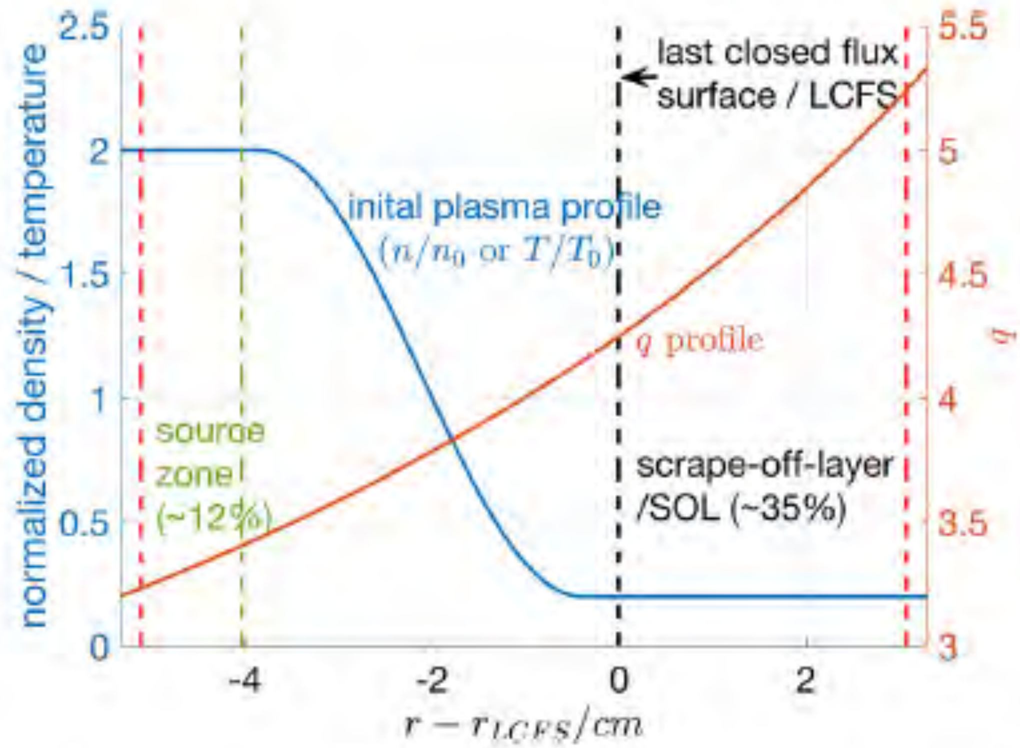

FIG. 1. Simulation setup in the radial direction at $t = 0$. Red dashed lines designate boundary zones; and green dashed lines indicate mass and heat source location.

Electrostatic Potential (e.g. streamlines for plasma turbulence)
Zoomed in view of inboard and outboard side of density fluctuations:

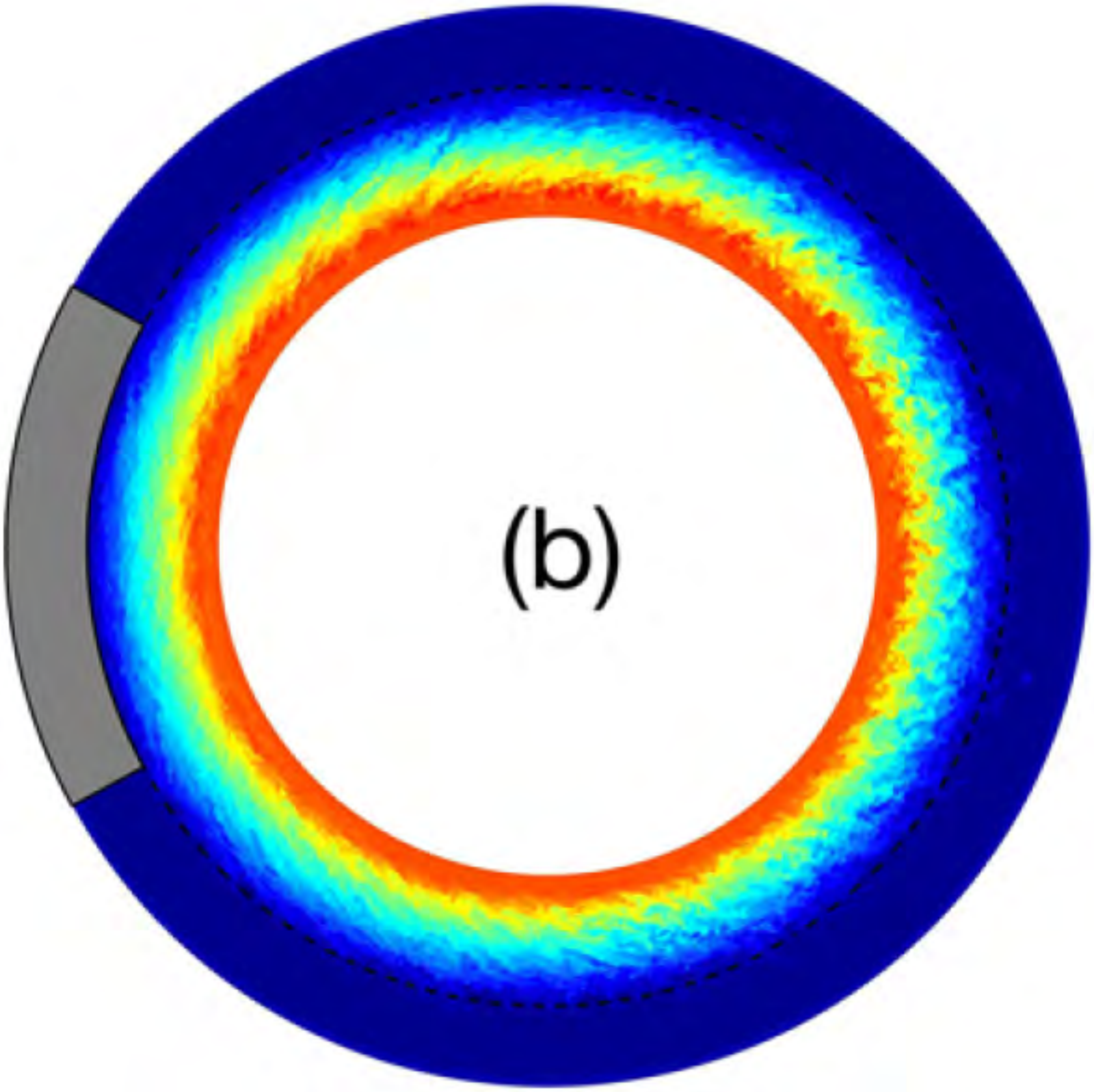
(b)

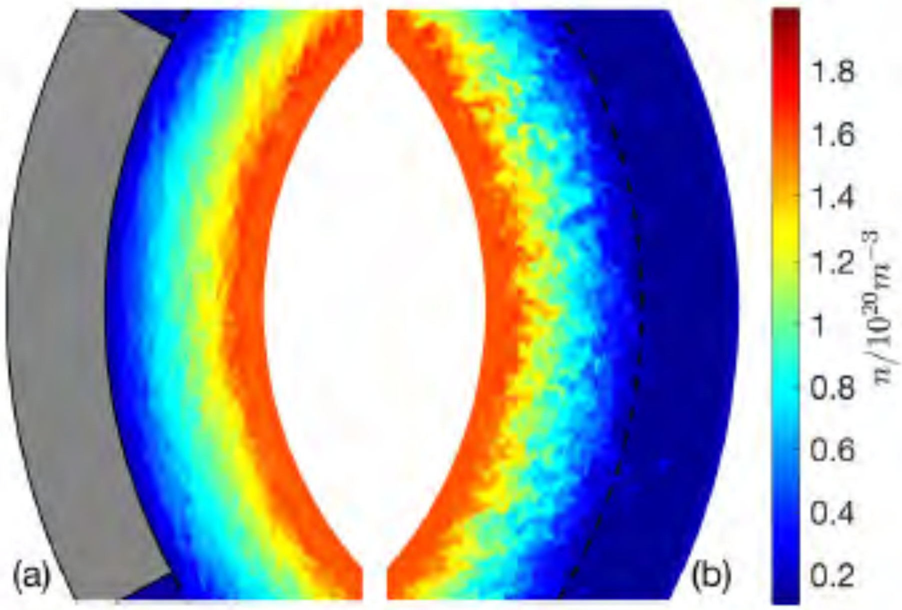

FIG. 4. (a) Inboard and (b) outboard portions of a poloidal snapshot of the density in the saturated stage.

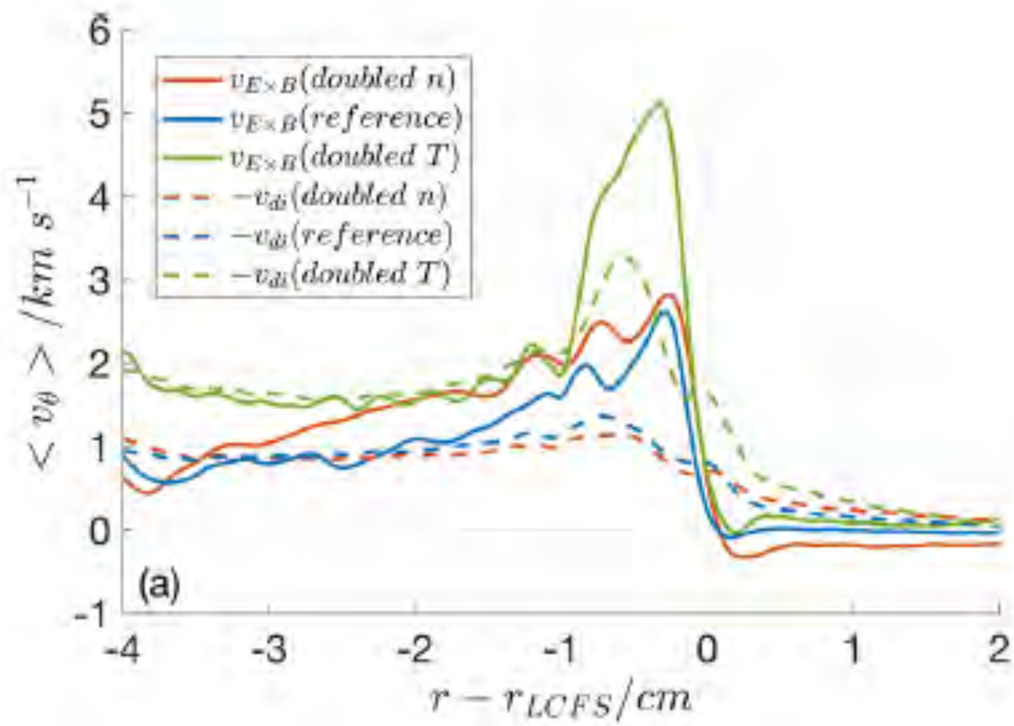

Turbulence amplifies the ExB shear flow at the LCFS. Higher temperatures with reduced collisional flow damping result in stronger ExB shear flow. Higher density with higher collisional flow damping results in weaker shear flow.

Turbulence is concentrated on the low-field side, resulting in creation of parallel ion flows to reconnect low-field and high-field sides. As a result, plasma pressure is NO LONGER A FLUX FUNCTION at the boundary region:

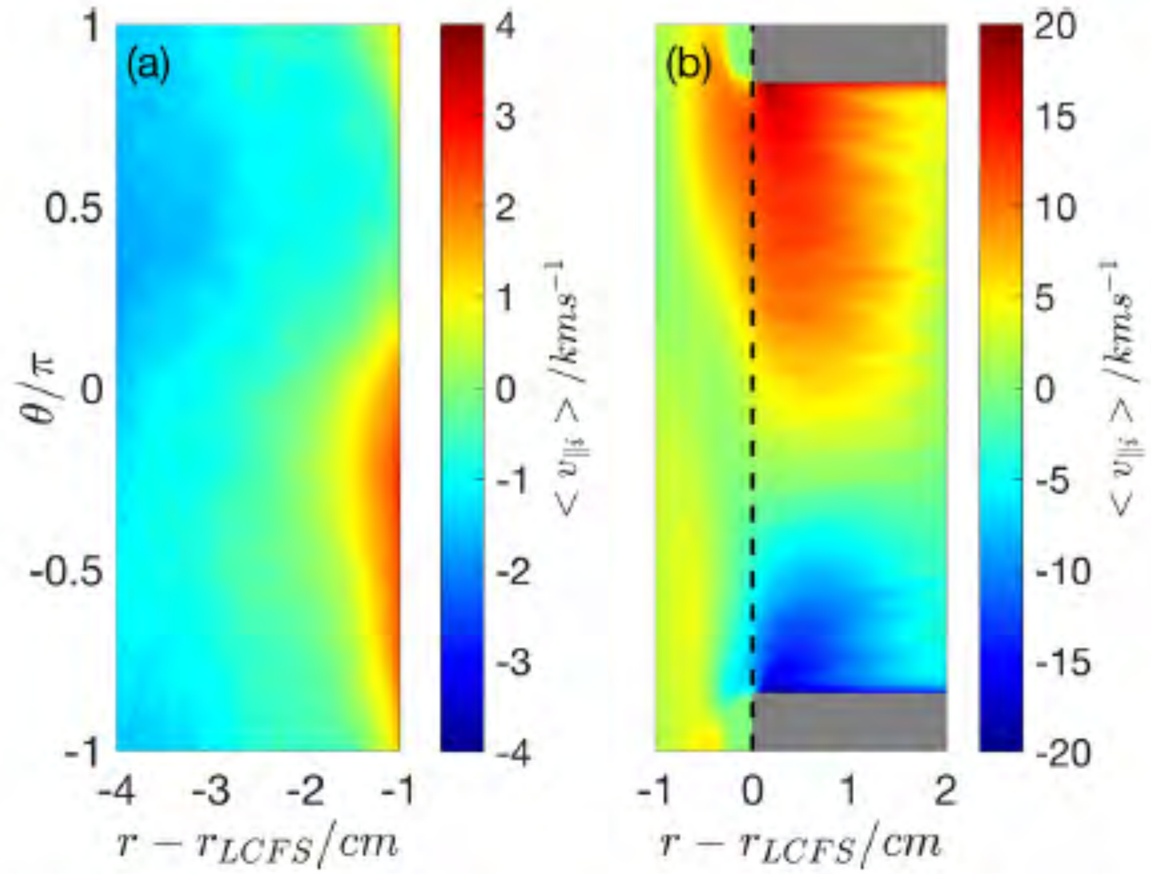

FIG. 22. Time and toroidally averaged $v_{\parallel i}$ in (a) inner closed-flux region and (b) near the LCFS and the SOL region for the doubled temperature simulation.

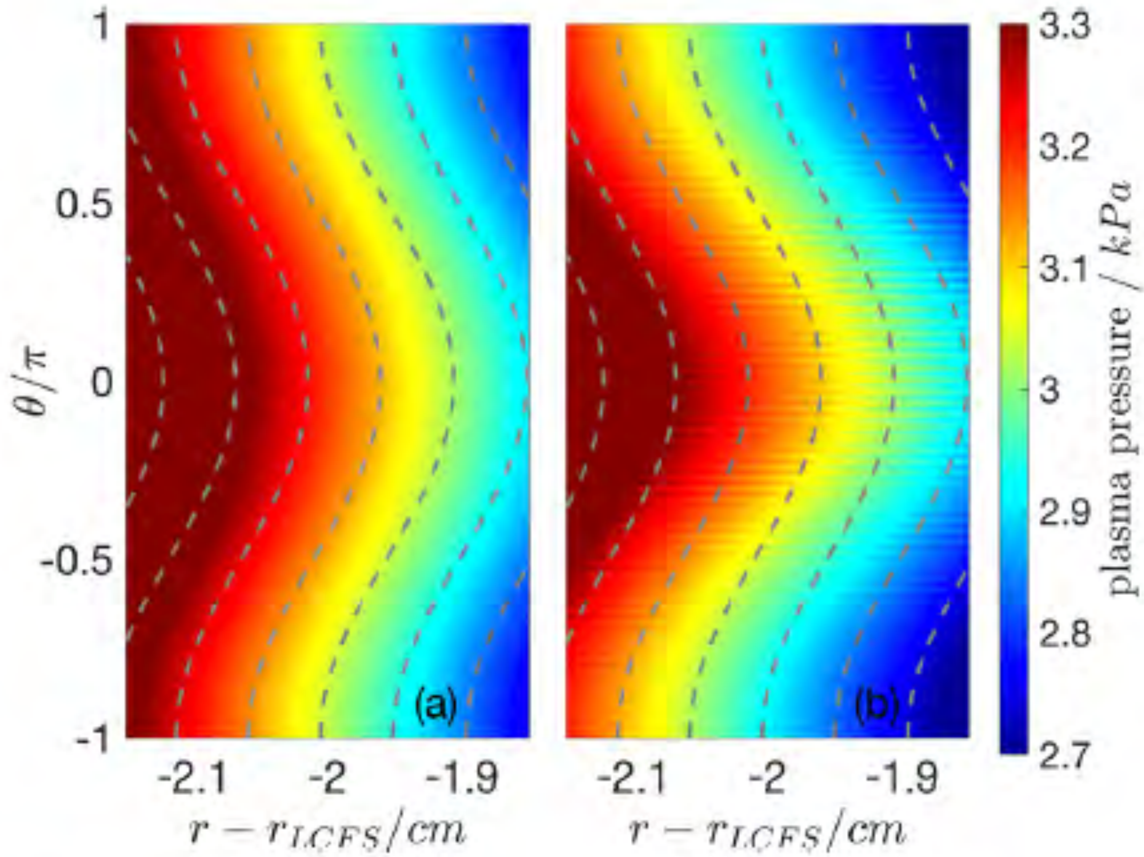

FIG. 24. Time-averaged pressure and flux contours (dashed) of (a) doubled temperature and (b) doubled density simulations.

These results give hints that the ExB shear flow (driven by turbulence) have an important role in the physics origin of the density limit and the L-H transition….

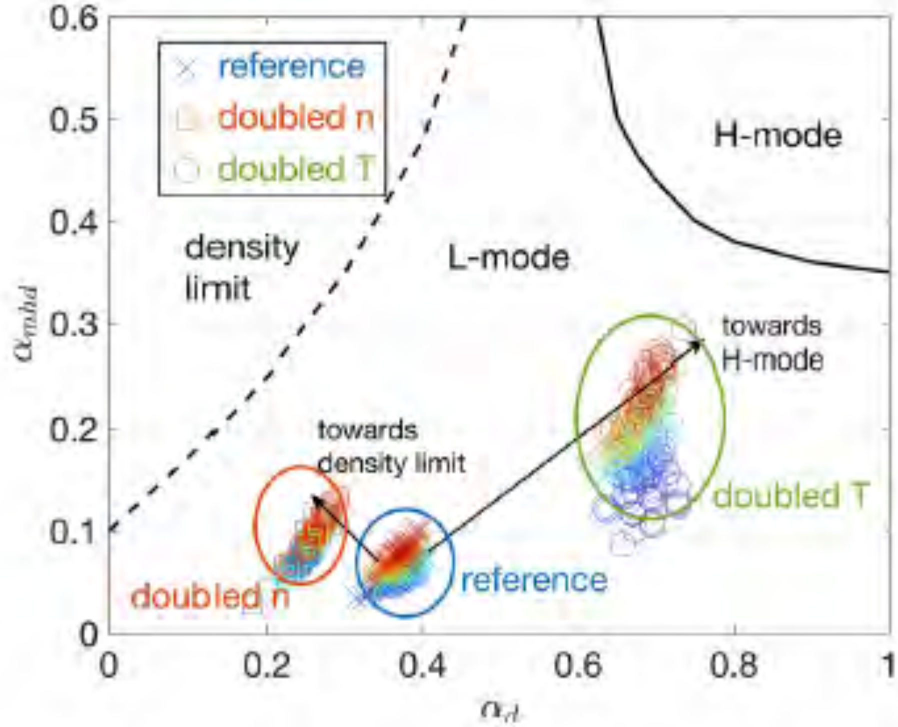

FIG. 9. $\alpha_d - \alpha_{mhd}$ phase space diagram and time evolution (blue to red) of doubled density (squares), reference L-mode (crosses), and doubled temperature (circles) simulations.

Flux-driven simulations of turbulence collapse

G. Y. Park,[1] S. S. Kim,[1] Hogun Jhang,[1] P. H. Diamond,[1,2] T. Rhee,[1] and X. Q. Xu[3]
[1]*National Fusion Research Institute, Daejeon 305-333, South Korea*
[2]*CASS and Department of Physics, University of California, San Diego, La Jolla, California 92093-0429, USA*
[3]*Lawrence Livermore National Laboratory, Livermore, California 94551, USA*

(Received 8 September 2014; accepted 27 February 2015; published online 12 March 2015)

Turbulent flux-driven simulations show formation of edge barrier with sufficient ion heat flux….

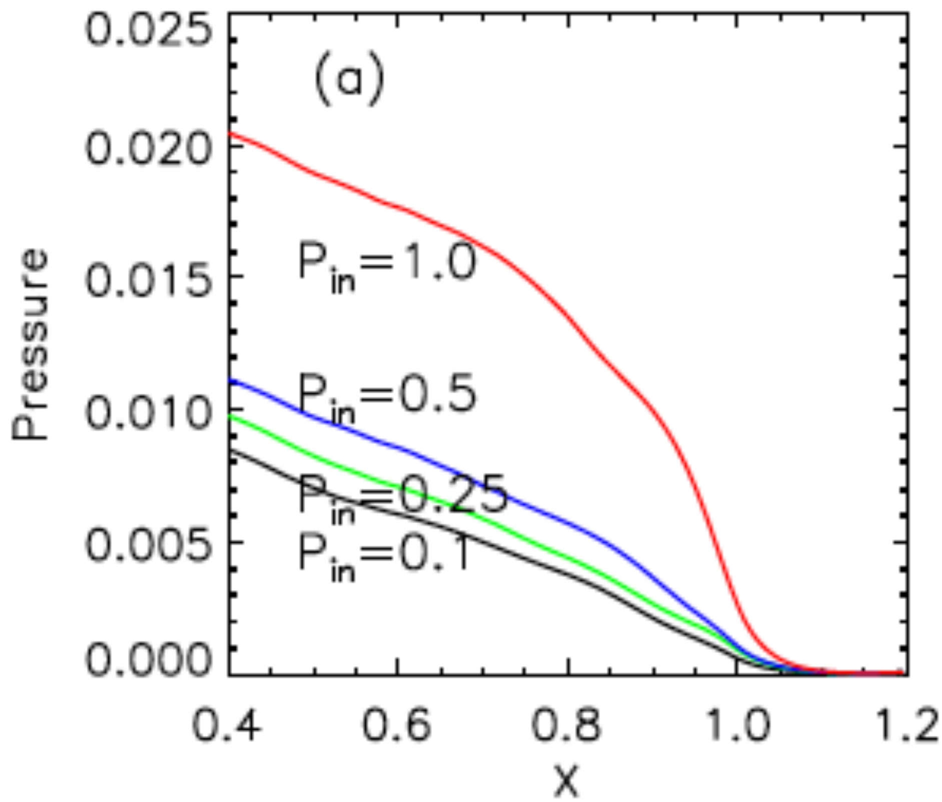

E.

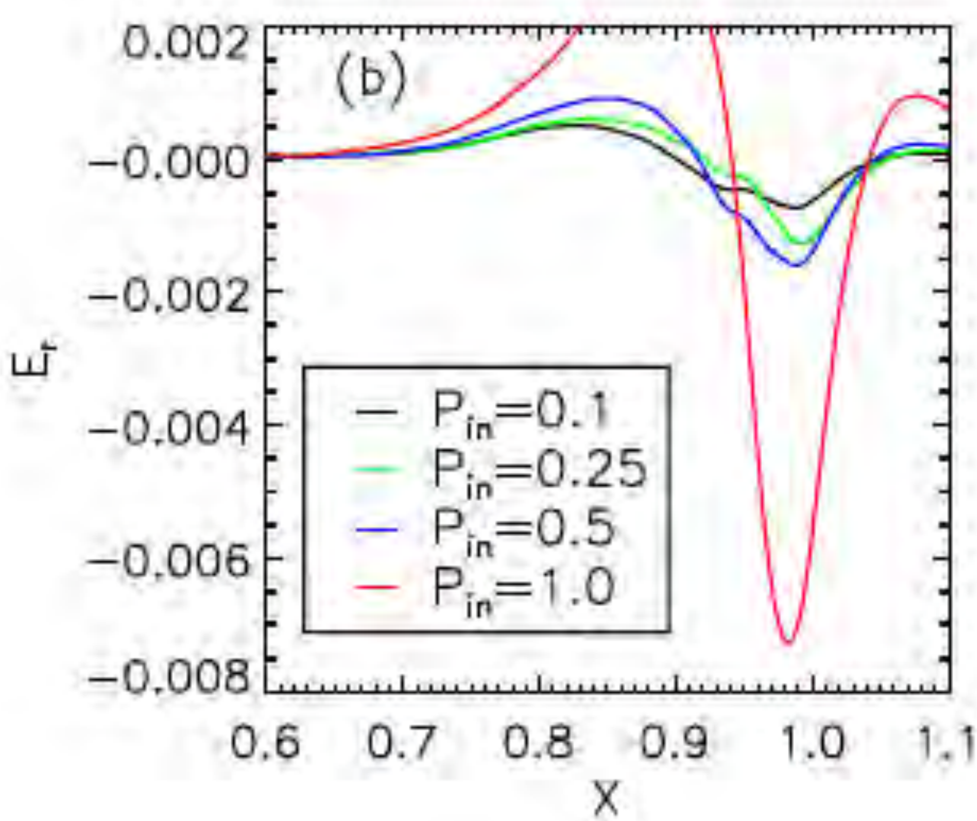
(b)
0.002
−0.000
−0.002
−0.004
−0.006
−0.008
E_r
P_{in}=0.1
P_{in}=0.25
P_{in}=0.5
P_{in}=1.0
0.6
0.7
0.8
0.9
1.0
1.1
X

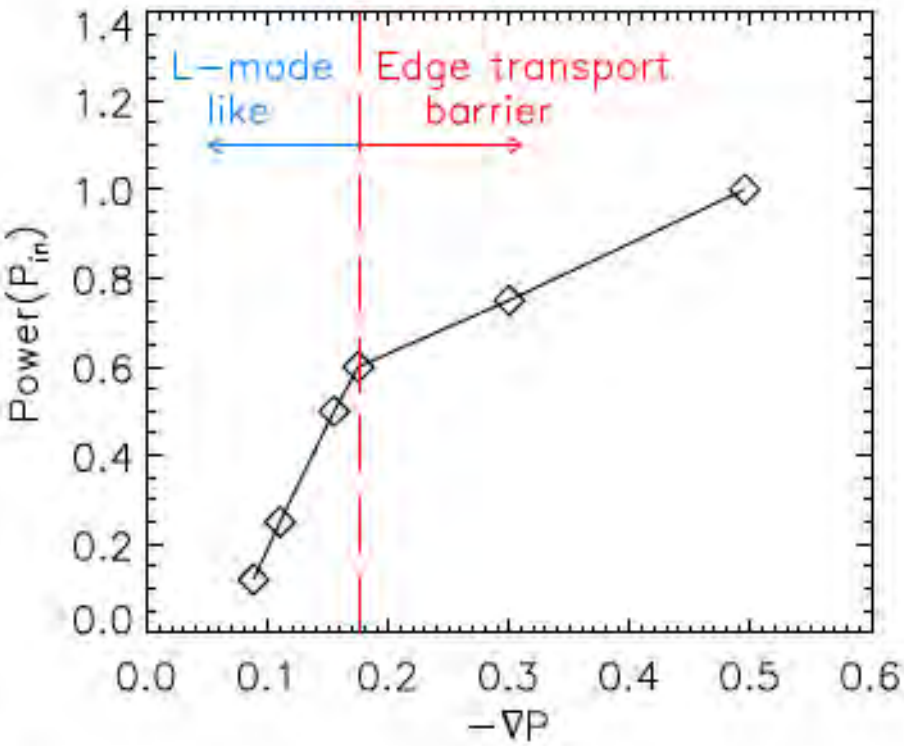

FIG. 3. Input power versus $-\nabla P$ showing a feature of the first order phase transition.

The rate of work done by turbulence on the ExB shear flow, normalized to the rate of energy input into the turbulence, appears to play a role in triggering the L-H transition

$$R_T = \frac{\langle \tilde{v}_r \tilde{v}_\theta \rangle \langle V^{LF}_{E\times B} \rangle'}{\gamma_{eff} \langle \tilde{v}^2_\perp \rangle},$$

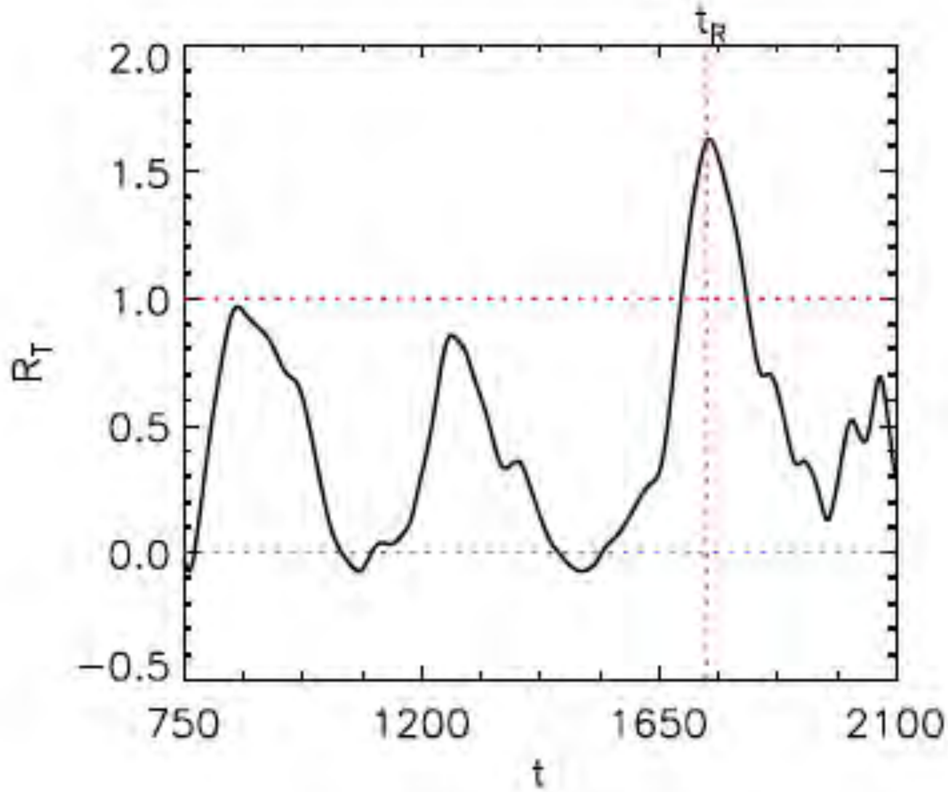

FIG. 5. Time traces of R_T at $x = 0.96$.

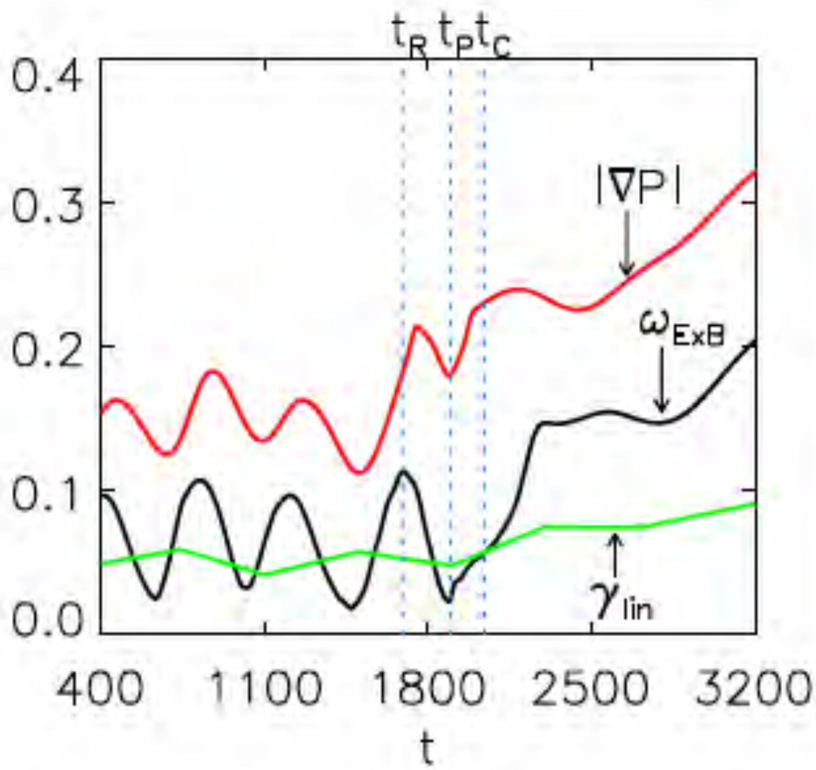

FIG. 6. Time traces of space and time-averaged $|\nabla P|$, $\omega_{E\times B}$, and γ_{lin} around the maximum radial point of $|\nabla P|$. $t = t_C$ denotes time when $\omega_{E\times B} > \gamma_{lin}$ is satisfied. Turbulence collapse occurs at t_R. Positive feedback between pressure gradient and mean flow shear begins at $t = t_P$.

3) PMI: effects of plasma on materials

a) Erosion via Physical, Chemical Sputtering

b) Plasma Ion Implantation & Diffusion, Trapping in Mat'l

c) Evolution / Degradation of Mat'l Properties

d) Heat Flux

4) Frontier Issues

a) Handling Heat Flux @ Diverter Target

- Detached / Radiative Diverter
- Negative Tri-Angularity
- Super-X
- Snowflake Diverter

b) Integrating (a) w/ High Perf. Core Plasma

See viewgraphs
for effects of
plasma on materials ...

3) PMI: effects of plasma on materials

a) Erosion via Physical, Chemical Sputtering

b) Plasma Ion Implantation & Diffusion, Trapping in Mat'l

c) Evolution / Degradation of Mat'l Properties

d) Heat Flux

4) Frontier Issues

a) Handling Heat Flux @ Divertor Target

- Detached / Radiative Divertor
- Negative Tri-Angularity
- Super-X
- Snowflake Diverter

b) Integrating (a) w/ High Perf. Core Plasma

4b (cont'd)

- adequate β
- low disruption provability
- n/n_G density limit
- No transient First Wall Coating (B, Li, ...)

c) Tritium Retention in Wall & Achieving TBR > 1

[Tritium Breeding Ratio]

d) Adequate First Wall & Diverter Lifetime

- Novel Solid Matl's ⊕ Adequately Small Heat Fluxes
- Liquid Walls?
  - Flowing?
  - Stagnant layer?
- "Spongy Solid" w/ Liquid Metal Embedded?